UCRL-52938

Wind-power site-screening methodology Final report

J. J. Walton

C. A. Sherman

J. B. Knox

Lawrence Livermore National Laboratory, University of California
Livermore, California 94550

October 1980

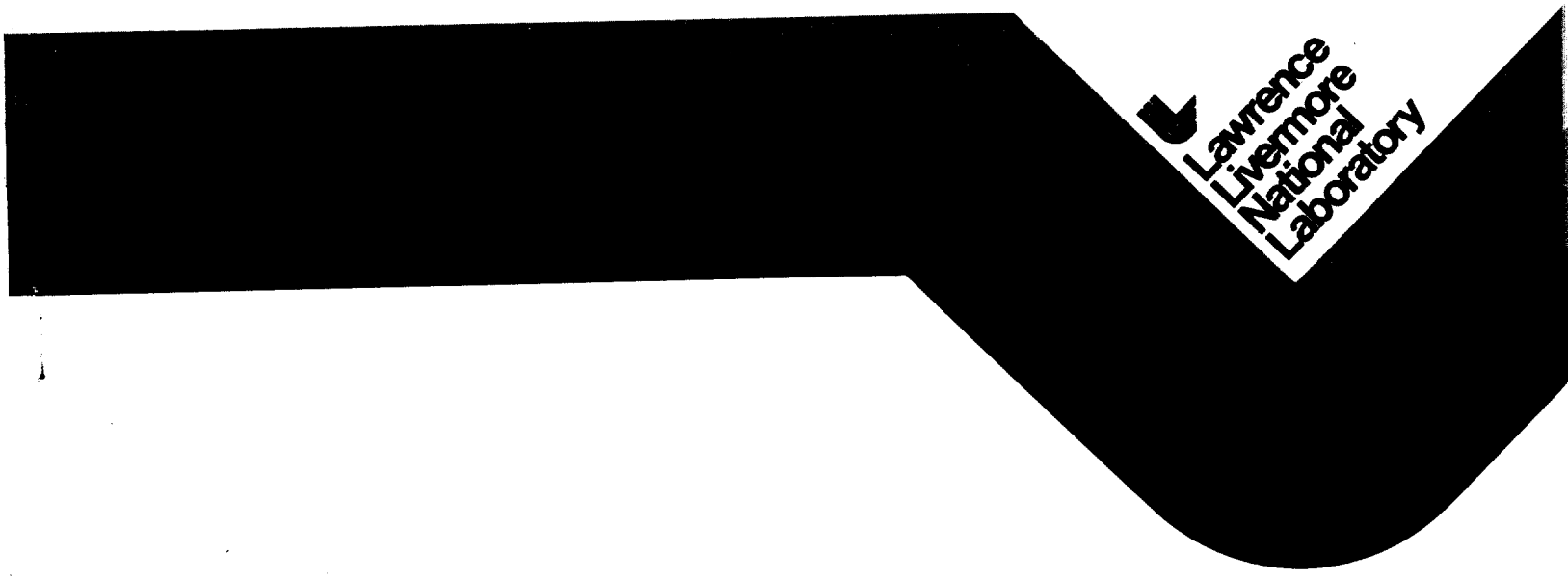

UCRL-52938
Distribution Category UC-11

Wind-power site-screening methodology Final report

J. J. Walton

C. A. Sherman

J. B. Knox

Lawrence Livermore National Laboratory, University of California
Livermore, California 94550

Manuscript date: October 1980

LAWRENCE LIVERMORE LABORATORY
University of California • Livermore, California • 94550

PREFACE

For several years, the technical leaders of the U.S. Wind Energy Program have recognized that there are two major prerequisites to the successful implementation of wind energy. The first is the emergence of an economical, reliable wind-turbine technology. The second pertains to techniques for locating sites of high wind potential for deploying these reliable technologies as they become available. An effective site-screening methodology contributes to the timely location and documentation of the wind resource even in the presence of complex terrain, where enhancement of the resource occurs. An effective methodology is one that leads to a better or more reliable identification of favored sites, thus improving the economics of operating wind systems. For example, if we could identifiy a site at which the wind is equal to or greater than the rated speed of a wind-turbine generator for one-half of the annual wind regime, it would indeed be a favored site.

We recognize that the Department of Energy (DOE) needs a spectrum of site-screening methodologies, from low-cost techniques that are perhaps more uncertain than desirable to more advanced site-screening methods with reasonable expectations of more reliable performance. By performance we mean the ability to identify the location, geographic extent, and a measure of the resource intensity (e.g., mean annual wind speed). This report describes such a methodology, its logical steps and components, and its verification against a two-year data base developed specifically for wind-energy purposes. The site-screening methodology, as developed, illustrated, and verified, is promising enough in performance to contribute to future DOE regional site-screening needs. It has been a pleasure to work with the Wind Energy Branch of the DOE during the past four years to bring this work to completion. In this regard, we appreciate the interest and support of Lou Divone, George Tennyson, and Carl Aspliden.

Joseph B. Knox, Division Leader, Atmospheric Science Division, LLL.

CONTENTS

ABSTRACT

In 1975, the Energy Research and Development Administration (ERDA) requested that the Lawrence Livermore Laboratory develop, validate, and demonstrate a wind-energy site-screening methodology suitable for defining the location, geographic extent, and strength of the resource. The appropriate core capabilities existing at that time, namely principal-components analysis techniques for classifiying types of regional flow fields, and a three-dimensional diagnostic flow model were blended into a rationale for screening wind sites in the presence of complex terrain. This report describes the relevant contributing capabilities, the developed screening methodology, the prospectors' preliminary wind-resource maps for the island of Oahu—generated to guide the development of the observational network, and the data base developed for testing. It also illustrates the use of the methodology on the island of Oahu and describes two annual assessments of Oahu's wind-energy potential. The methodology, tested on an independent set of several stations withheld from model development, is shown as able to identify wind-energy resources created by terrain enhancement quite well, with the annual mean wind speed for the independent data set depicted within about 1 m/s for a reasonable range of annual wind speeds.

INTRODUCTION

The Department of Energy (DOE) Wind Systems Branch needs a spectrum of wind-energy prospecting techniques extending from low-cost techniques that are perhaps more uncertain than desirable to more advanced methods with reasonable expectations of more reliable performance. The intent of wind-energy site screening is to identify the location, geographic extent, and strength of a wind-energy resource. Ideally, a modern wind-energy prospector would have a choice of techniques available for any given application. The screening methodology selected would depend on many factors: the suspected magnitude of the resource, the terrain in which the resource is believed to exist, the time available for assessment, the degree of accuracy desired in the wind-energy resource assessment, and the resources available or appropriate for the assessment. This report summarizes the applied research performed by the Lawrence Livermore Laboratory (LLL) to develop and validate an advanced wind-energy site-screening methodology and to illustrate this methodology in regard to the assessment of the large wind-energy resource of the island of Oahu.

In 1976 the National Wind Energy Program asked LLL to help develop and validate an advanced site-screening methodology for wind-energy resources.

In the presence of complex terrain, existing meteorological data bases are frequently inadequate for identifiying and documenting the extent, strength, and characteristics of the wind resource created, in many instances, by terrain enhancement. Indeed, the traditional meteorological data available on Oahu a few years ago was no exception. In 1975, and certainly by early 1976, Oahu was recognized as an outstanding test bed for a regional-scale site-selection methodology. As a result, our LLL team was invited to join in the regional quest for wind resources. The core capabilities involved in the LLL site-screening methodology include (1) three-dimensional, diagnostic flow simulations over complex terrain, (2) modern statistical techniques of pattern recognition, which have been adapted to regional wind fields and, to very limited extent, (3) remote sensing of atmospheric wind fields by laser scintillation.

SITE-SCREENING METHODOLOGY

The logic flow and steps in the LLL site-screening methodology are as follows (Knox, 1980):

Step 1. Wind measurements

This step involves the acquisition and data-basing of all surface and upper-air wind data from climatological sources for the region of interest. Available sources of information from special networks (e.g., the University of Hawaii observational studies) are also obtained. In normal wind-prospecting and site-selection situations, such special studies are frequently nonexistent.

Step 2. Model Inputs

At least one year of input is abstracted from the data base to type the annual set of regional hourly flow patterns so that the annual wind regime can be represented by a finite number of typed days and their frequency distribution.

Step 3. Principal Components Analysis

LLL has developed statistical methods of pattern recognition for regional flow fields, using principal-components analysis (PCA). The PCA model provides the time-dependent coefficients of the empirical eigenvectors for each typed day as well as the frequency distribution of typed days in the data set. This information is stored in "Fitted day data for each type" and in "Sequence of day types," respectively.

Step 4. Three-dimensional regional winds

Diagnostic regional-flow calculations are performed for each typed day, say at three hourly intervals, by means of the MATHEW computer model, using the model inputs (Step 2) and detailed terrain boundary conditions. Hence, the spatial distribution of wind energy in the region is obtained for each typed day.

Step 5. Annual wind-energy potential

The regional, annual wind-energy potential is calculated from Step 4 and from information on the day-type frequency distribution.

In early 1976, before any significant result from special measurement programs, it was desirable to obtain early estimates of the location, strength, and extent of the wind resources on the island of Oahu. The data available for this purpose were from the surface stations operated by the National Weather Service (NWS), from the military services, and from upper-air observations done on the windward side of Oahu during World War II. All of this information came from stations at low elevations associated with aviation or agricultural activities. From the five-year data set, we abstracted they wind data for 1400 LST, and we constructed a composite of the most frequent wind direction and speed for each station. The rationale for this choice in 1976 was that, since the trade wind flows are repetitive and very frequent, subregions of high wind potential should be defined in regard to location in simulations of the composite day. This rationale would,

obviously, have to be modified for preliminary screening simulations in nontradewind areas. For instance, if there were more than one dominant regional flow pattern, in a given region more than one preliminary simulation would be performed for the initial mapping of preferred locations.

This data set was used as model input to the MATHEW regional-flow model, whose output was wind speed and schematic streamlines 150 m above terrain. These "wind-prospector maps" showed speed maxima on the corners of the island of Oahu, with minima in the central valley and immediately up and downwind of major topographic barriers. The area of Kaena point required special treatment because the fine structure of the topography was not represented properly by 1000-m averaged topography. By "zooming-in" on Kaena point with a subregional calculation, using 0.5-km grid spacing, promising wind maxima of small spatial dimensions were indicated. Wind maxima were found on the Kahuku hills in the northeast portion of the island which was devoid of climatological measurements. The relatively simple topography of the Kahuku area, in comparison to other more rugged features of Oahu, suggested that a site-screening methodology and component models could be reliably tested there. This wind resource if more adequately documented, was also judged to be of major significance to the island of Oahu.

These wind-prospector maps, along with the finer-scale calculations for Kaena and Kahuku areas, contributed to the positioning of the LLL wind-measurement stations: Laie measured the trade winds immediately upwind of the Kahuku area; Kahuku Hill (300 m above sea level) measured the wind (10-m above terrain) in or near the wind maximum; Waialua characterized the flow upwind of the Kaena Point terrain; and Mokuleia was located near one of the indicated wind maxima on Kaena Point. Data from this four-station network, along with data from nine well-exposed stations sited by the University of Hawaii and eight stations operated by the NWS and the military, were incorporated into the Oahu data base for August 1976 — July 1978.

By September 1976, the stage was set for the acquisition of a regional data base of wind information designed specifically for testing wind-prospecting methods. The next two years were devoted to data acquisition, data basing, and some interim wind-energy assessments that served as provisional tests of the site-screening techniques being developed. From Fall 1978 to the projected close of the project in June 1979, the two-year data base was used in regional assessments of wind energy, and the developed methodology was tested against a subset of the data base reserved for validation.

The remainder of this report describes the LLL site-screening methodology in detail, the primary capabilities that contribute to the screening methodology, the data base used in the validation, and the results of the wind-energy assessment of the island of Oahu.

Data for the more-detailed analysis are for the two-year period August 1976—July 1978 and were provided by cooperating agencies, such as the NWS, the military, the University of Hawaii, and the four sites instrumented by LLL. The data consist of hourly average wind speed and direction. Table 1 lists these measurement stations, their locations and elevations, the agency supplying the data, and a two-letter designator (code) for each. The locations of the stations are shown

TABLE 1. Oahu data-base surface observation stations.

	Code	UTM coordinates km		Ground level, m ASL	Instrument height, m AGL
		North	East		
LLL stations					
Mokuleia	MN	2383.18	583.06	609	15
Waialua	WR	2386.51	590.52	5.5	15
Kahuku Hill	KH	2396.68	603.17	300	10
Laie	LT	2394.83	610.74	3	26
Permanent stations					
Barbers Point NAS	BP	2355.98	595.48	3	3
Wheeler AFB	WH	2375.90	599.48	250	3.7
Comsat Corp. -Paumalu	CS	2396.98	599.84	137	15
Honolulu Airport-NWS	HA	2358.27	612.50	2	7.6
Kaneohe MCAS	KM	2373.02	626.40	2	4.5
Kaena Point-SAMTEC	KP	2386.01	575.65	270	7.6
Pearl Harbor-FWC	PH	2361.63	609.30	3	11
Mauna Kapu-USN	MK	2366.58	592.88	782	23.2
University of Hawaii stations					
Kahuku Opana	KO	2398.80	602.20	162	14
Koko Head	KK	2352.57	634.36	195	11
Maunawili	MW	2361.86	627.54	125	9
Mauna Kapu	MU	2367.14	593.18	825	12
Helemano	HE	2382.15	601.15	336	14
Tantalus	TT	2360.20	622.80	596	21
Kolekole Pass	KL	2375.28	591.60	527	29
Kaena Point Tower	K3	2384.93	577.54	385	9
Kahuku Road	KR	2399.37	603.04	12	10

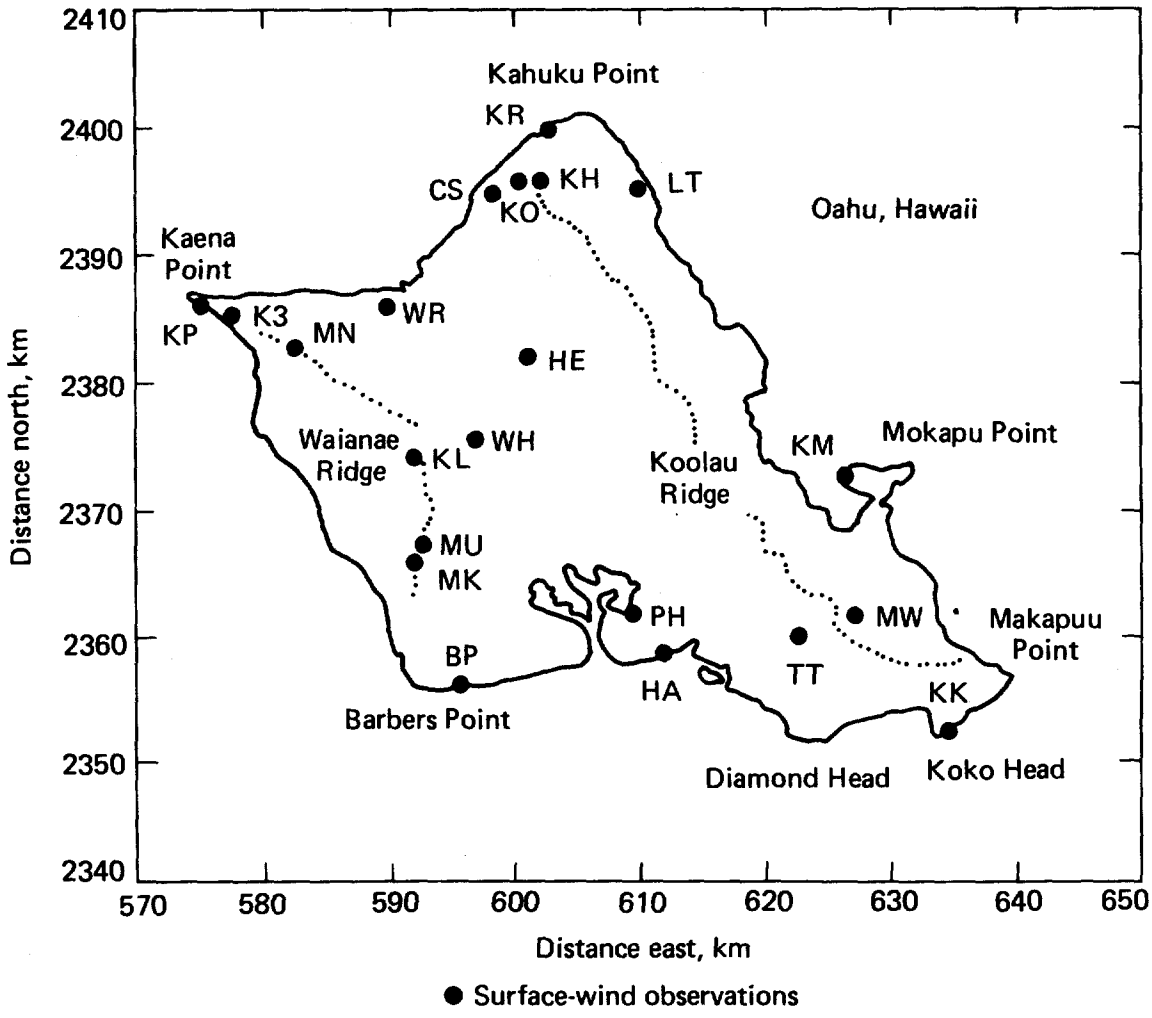

FIG. 1. Sites providing surface-wind measurements for the LLL surface-wind data base.

on the map of Oahu in Fig. 1. Not all stations reported for the full two-year period, and no station had 100% reporting reliability. A summary of these data may be found in the LLL Oahu surface. Wind network summary of data, August 1976 through July 1978 (Shinn et al, 1979).

We begin by stating the premises that are the basis for the site-screening methodology, describe the objective analysis codes through which these are premises implemented, and proceed to a study of wind potential based on the two years of data. Because of changes in station operation and availability, the study of wind potential for the two annual periods will be done seperately. This will also provide some information on the year-to-year variability of wind potential.

SCREENING PREMISES

The foundation of site-screening methodology rests on our ability to identify recurrent temporal and spatial wind-field patterns and to predict winds with objective diagnostic models. Specifically, the premises on which the Oahu siting analysis is based are as follows:

- Recurring patterns will be observed in the diurnal behavior of the wind field over the region for one month. The month can then be represented by a few subsets of days with similar diurnal patterns. (In this study, data for both years were described by a single subset for each of the 12 months. Days unlike those in the subset were not included in the subsequent analysis.)

- Because all days in a subset are similar, we assume that a subset of days for a given month of data can be replaced by a single typical day. Weighted averages of these days will give the same statistics as those for the monthly subsets.

- Statistical information can be inferred at locations without data by using MATHEW predictions based on input from the typical day representing each month.

OBJECTIVE ANALYSIS CODES

Before discussing the above points in more detail, we consider the problems of reducing and approximating large data sets of vector observations and of objectively estimating wind speed and directional information at locations where observations are nonexistent.

OBJECTIVE IDENTIFICATION OF TYPICAL WIND PATTERNS

To determine the main characteristics of regional wind-field patterns, we need a process that reduces the large groups of data. We have selected PCA as the basis of this process. PCA produces a complete set of orthogonal eigenvectors representing the original data from which the original data may be expressed. Some advantages of this representation are:

- The eigenvectors and principal components are determined from the original data and derived by an objective mathematical procedure.
- The relative magnitudes of eigenvalues can be used to rank-order the eigenvectors in terms of how well they represent the data.
- The most significant eigenvectors can be identified with physically important patterns in the original data.
- The primary eigenvectors provide a highly efficient basis set for approximating the original observed data.

A summary of the PCA technique and the formal procedures of empirical eigenvector analysis, as used previously in atmospheric science, is given by Essenwanger (1976). Hardy (1977) has extended the PCA technique, which was applied originally to scalar quantities, to vector fields. A detailed discussion of this technique and its application to wind-field data is found in Hardy and Walton (1978).

The eigenvector expansion coefficients resulting from PCA can be used for an objective comparison of wind fields on different days throughout a period of interest (Walton and Hardy, 1978; Walton and Sherman, 1978). Once subgroups of similar days have been identified, the expansion coefficients can be used to generate wind patterns typical of these subgroups and to establish, day by day, the quality of the fit.

The data to be analyzed consist of horizontal wind velocities measured simultaneously at a number of geographic locations. These data are represented as complex numbers. Each observation consists of a measured wind speed and direction. By use of complex notation, the observed two-dimensional velocity v is associated with a complex number

$$\sigma = se^{i\theta} \quad , \tag{1}$$

where s is the wind speed and θ is the direction. If observations are made at N different geographic locations and M different times, the data may be organized into an N x M rectangular matrix $\underset{\sim}{S}$. The elements of $\underset{\sim}{S}$ are

$$s_{km} e^{i\theta_{km}},$$

where k = 1, N < M denotes the location of the observation and m = 1, M, the time of the observation. An N x N hermetian matrix $\underset{\sim}{H}$ can be defined in terms of $\underset{\sim}{S}$ as follows:

$$\underset{\sim}{H} = \underset{\sim}{S}^{\dagger} \underset{\sim}{S}/M, \tag{2}$$

where $\underset{\sim}{S}^{\dagger}$ is the complex conjugate transpose of $\underset{\sim}{S}$. Using standard mathematical procedures the N eigenvalues, λ_k (real), and N eigenvectors, $\hat{E}_k$ (complex) of $\underset{\sim}{H}$, can be calculated. The eigenvectors have the property

$$\underset{\sim}{H}\, \hat{E}_k = \lambda_k \hat{E}_k, \qquad k = 1, N \tag{3}$$

and satisfy the orthonormality condition

$$\hat{E}_j^{\dagger} \cdot \hat{E}_k = \delta_{jk} \ . \tag{4}$$

The primary eigenvector for August 1976 is illustrated in Fig. 2.

The N eigenvectors form a complete orthonormal basis set in N-space. As such, they can be used to expand the data at each time when the observations are written as an N-dimensional complex vector $\vec{S}_m$. It follows from Eq. (4) and the completeness of the set that

$$\vec{S}_m = \sum_{k=1}^{N} c_{km}\ \hat{E}_k, \qquad m = 1, M \tag{5}$$

where

$$c_{km} = \hat{E}_k^{\dagger} \cdot \vec{S}_m \ , \qquad k = 1,N; \quad m = 1, M \ . \tag{6}$$

Figure 3 shows an example of the expansion coefficients for the first eigenvector for the first six days of August 1976.

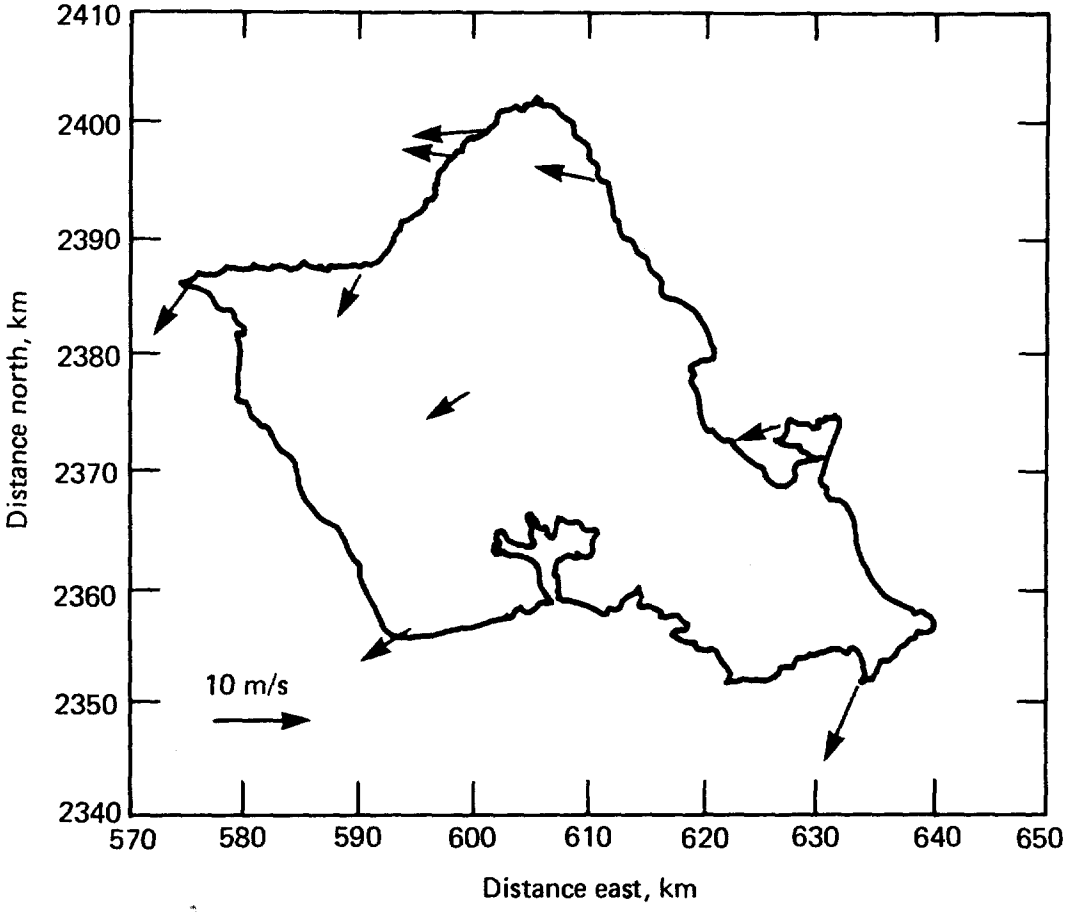

FIG. 2. Primary eigenvector for August 1976, from data on the island of Oahu, Hawaii.

The expansion coefficients (principal components) c_{km} are unique and generally complex. They constitute a scaling and rotation of the elements if $\hat{E}_k$. The mean square of the expansion coefficients of eigenvector k can be shown to equal the eigenvalue associated with that eigenvector.

$$\left(\sum_{m=1}^{M} | c_{km} |^2 \right)/M = \lambda_k, \qquad k = 1,N. \tag{7}$$

In practice, the eigenvalues usually differ significantly in size. Eigenvectors corresponding to the largest eigenvalues are the primary spatial eigenvectors derived objectively from the observations. As stated above, they exhibit the spatial characteristics of the dominant wind-field patterns.

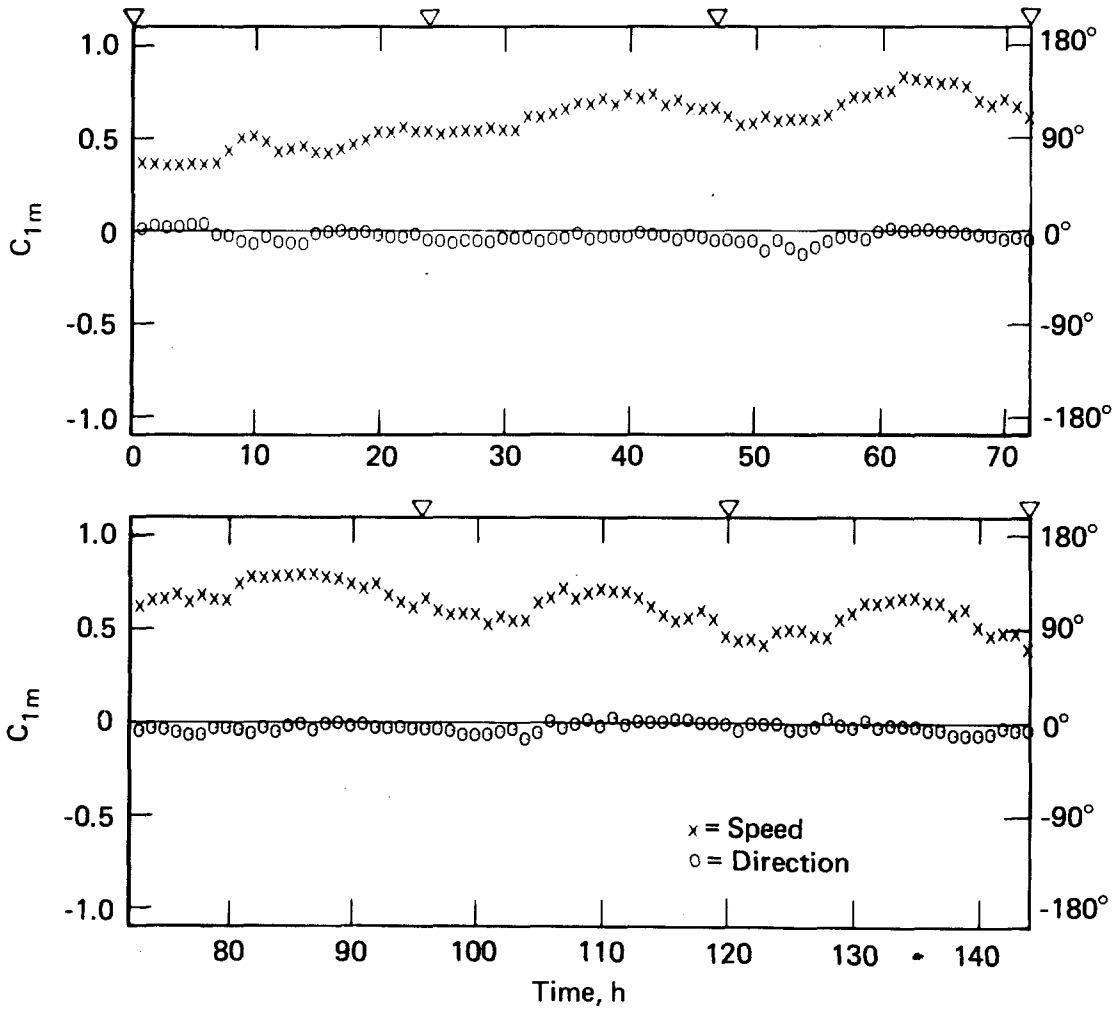

FIG. 3. Primary eigenvector expansion coefficients for the first six days of August 1976, from data for Oahu, Hawaii.

If the observed data contain recurrent temporal variations (eg. diurnal changes), the expansion coefficients c_{km} reflect these temporal patterns. These expansion coefficients may then be examined objectively to obtain groupings of days with similar temporal characteristics. Note in Eq. (2) that $\underset{\sim}{H}$ is unnormalized. Therefore, wind strength, as well as frequency, will contribute to the characteristics of this matrix. Hence, in the subsequent analysis, windier days will have greater influence than days with weak winds.

The first step in this process is to compare each day with all others for the period of interest (say a month). Since the first eigenvector exhibits the major features of the wind field, its expansion coefficients alone are used in the comparison. Two days are said to have similar characteristics if their expansion coefficients are the same, within prescribed error limits, for some fraction of the day. When the subgroupings of days have been defined, a typical day may be computed for each.

Consider a subgroup of L similar days. For a specified hour each day the wind fields are denoted by an observation vector $\vec{S}_m$. Writing the exansion coefficients for $\vec{S}_m$ in cartesian form,

$$c_{km} = x_{km} + i\, y_{km} . \tag{8}$$

Substitution into Eq. (5) gives

$$\vec{S}_m = \sum_{k=1}^{N} (x_{km} + i\, y_{km})\, \hat{E}_k . \tag{9}$$

We wish to approximate the L observations $\vec{S}_m$ by a single typical observation $\vec{T}$ that can also be expressed in terms of the $\hat{E}_k$.

$$\vec{T} = \sum_{k=1}^{N} (u_k + i\, v_k)\, \hat{E}_k . \tag{10}$$

The difference between $\vec{T}$ and $\vec{S}_m$ is a vector in N-space, representing the error between the approximation and the observation on day m:

$$\vec{D}_m = \vec{T} - \vec{S}_m . \tag{11}$$

The approximation $\vec{T}$ is said to be a best fit to the L observations $\vec{S}_m$ when the square of the magnitude of $\vec{D}_m$ averaged over all L days is minimized. One constraint is added: the mean square speed of the approximation must equal the mean square speed of the observation. The approximation is obtained by variational methods and has the form

$$u_k = \bar{x}_k \left[\sum_{j=1}^{N} (\overline{x_j^2} + \overline{y_j^2}) \Big/ \sum_{j=1}^{N} (\bar{x}_j^2 + \bar{y}_j^2) \right]^{1/2} \tag{12a}$$

and

$$v_k = \bar{y}_k \left[\sum_{j=1}^{N} (\overline{x_j^2} + \overline{y_j^2}) \Big/ \sum_{j=1}^{N} (\bar{x}_j^2 + \bar{y}_j^2) \right]^{1/2} , \tag{12b}$$

where the bar denotes an average over the L days within the subgroup. Fig. 4 shows the hourly expansion coefficients for the first eigenvector for the primary typical day representing August 1976. In subsequent analyses, one can use either the computed typical day or any day of the month that looks like it. The advantage of

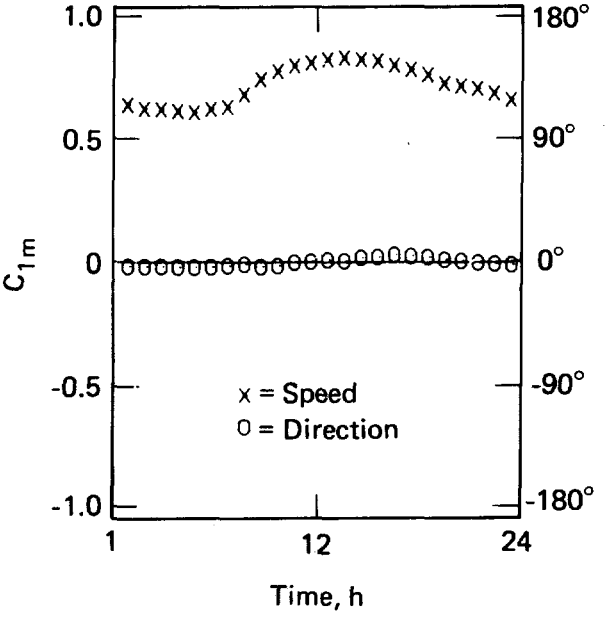

FIG. 4. Primary eigenvector expansion coefficients for the typical day representing August 1976 for Oahu, Hawaii.

using the typical day, instead of an actual one, is that large excursions at some sites would be smoothed out in computing the typical day. On the other hand, should we choose a day that looks like the typical day, we would have access to specific upper-air data, which can only be approximated for the computed day. For the analysis reported here, we chose to use, for each month, an actual day that closely resembles the computed typical day. In regions other than Oahu, where drainage winds and sea-breeze effects may be more important, the PCA techniques for identifying typical days are still useful if spatial correlation and organization exist. More-recent work indicates, that even with additional complications in the processes, spatial organization is reflected in the first eigenvector and in its time-dependent coefficients.

OBJECTIVE INTERPOLATION OF WIND-FIELD DATA

Early in the site-screening process, wind data may not exist at all points that show promise for wind energy. Thus a method to objectively estimate winds at these points is needed. To this end, we have used the MATHEW model developed by Sherman (1978). Based on the work of Sasaki (1958, 1970a,b), The program requires that deviations of winds estimated from observations be minimized (adjusted) in the least-squares sense while satisfying the condition of nondivergence.

In three dimensions, the function is defined as

$$E(u,v,w,\lambda) = \int_V \left[\alpha_1^2 (u - u^o)^2 + \alpha_1^2 (v - v^o)^2 + \alpha_2^2 (w - w^o)^2 \right.$$

$$\left. + \lambda \left(\frac{\partial u}{\partial x} + \frac{\partial v}{\partial y} + \frac{\partial w}{\partial z} \right) \right] dxdydz, \tag{13}$$

where x and y are the horizontal directions and z is the vertical direction; u, v, and w are the adjusted velocity components in the x, y, and z directions, u^o, v^o, and w^o are the corresponding observed variables. $\lambda(x,y,z)$, not to be confused with the eigenvalues discussed above, is the Lagrange multiplier; and the α_i are the Gaussian precision moduli reflecting observation errors and/or deviations of the observed field from the desired adjusted field. The associated Euler-Lagrange equations which, with the nondivergent constraint, minimize Eq. 13 are

$$2 \alpha_1^2 (u - u^o) + \frac{\partial \lambda}{\partial x} = 0 \tag{14}$$

$$2 \alpha_1^2 (v - v^o) + \frac{\partial \lambda}{\partial y} = 0 \tag{15}$$

and

$$2 \alpha_2^2 (w - w^o) + \frac{\partial \lambda}{\partial z} = 0 \quad , \tag{16}$$

with the nondivergent condition

$$\frac{\partial u}{\partial x} + \frac{\partial v}{\partial y} + \frac{\partial w}{\partial z} = 0 \tag{17}$$

Differentiating and using Eq. 17 gives the equation for ,

$$\frac{\partial^2 \lambda}{\partial x^2} + \frac{\partial^2 \lambda}{\partial y^2} + \left(\frac{\alpha_1}{\alpha_2} \right)^2 \frac{\partial^2 \lambda}{\partial z^2}$$

$$= -2 \alpha_1^2 \left(\frac{\partial u^o}{\partial x} + \frac{\partial v^o}{\partial y} + \frac{\partial w^o}{\partial z} \right) . \tag{18}$$

Boundary conditions become conditions on either λ or its normal derivative

$$\frac{\partial \lambda}{\partial n} = \left(\frac{\partial \lambda}{\partial x}, \frac{\partial \lambda}{\partial y}, \frac{\partial \lambda}{\partial z} \right) .$$

In the first case, if $\lambda = 0$, an open or "flow-through" condition pertains. If $\partial\lambda/\partial n = 0$, then no adjustment of the field takes place on the boundary. Given the solution of Eq. 18, Eqs. 14-16 provide u, v, and w in terms of known quantities.

Figures 5 - 7 illustrate the steps in this process. Figure 5 gives the observational data provided as input to MATHEW. These data are interpolated onto the MATHEW grid, producing an initial flow pattern in three dimensions. Figure 6 shows flow lines and isotachs of this interpolated field 60 m above topography. Strong divergences and convergences are often present in this field. Finally, after adjustment, a nondivergent field will result as shown in Fig. 7, where we again see flow lines and isotachs at 60 m.

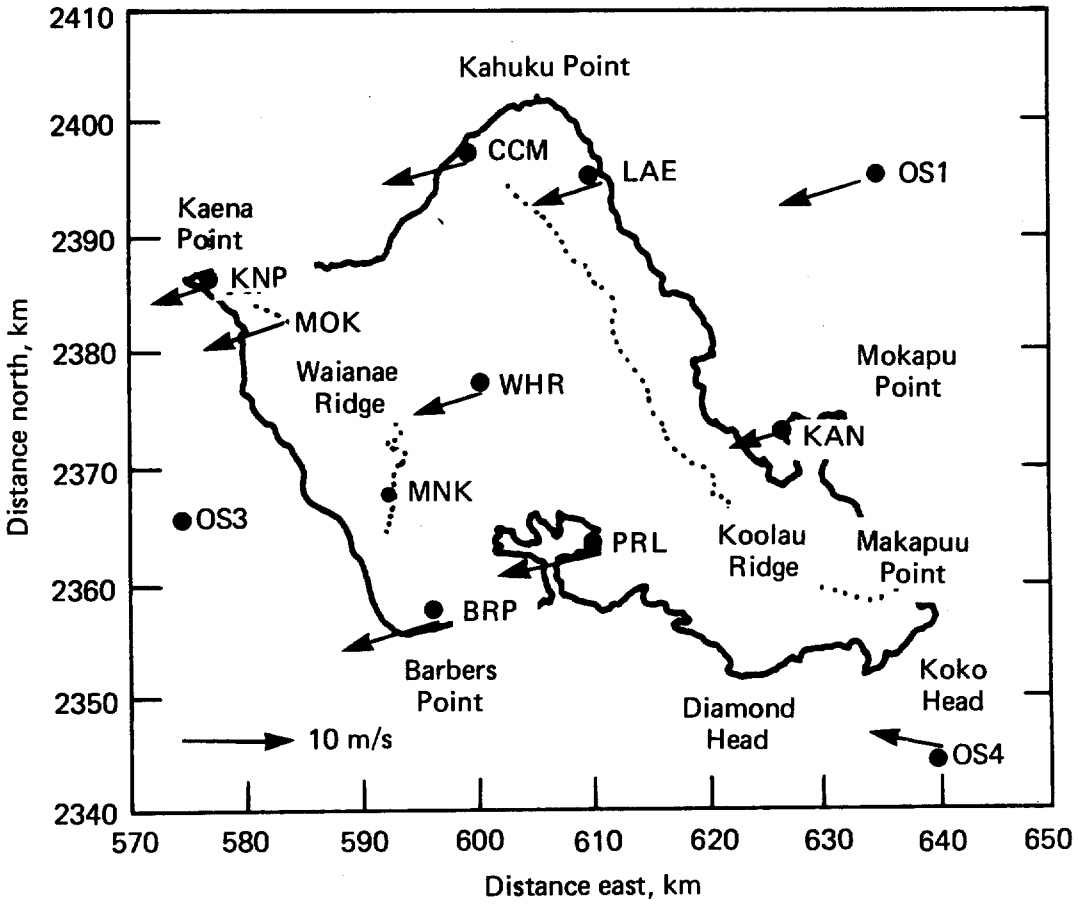

FIG. 5. Wind-velocity data adjusted to a common reference level of 60 m above topography, using a 0.2 power law.

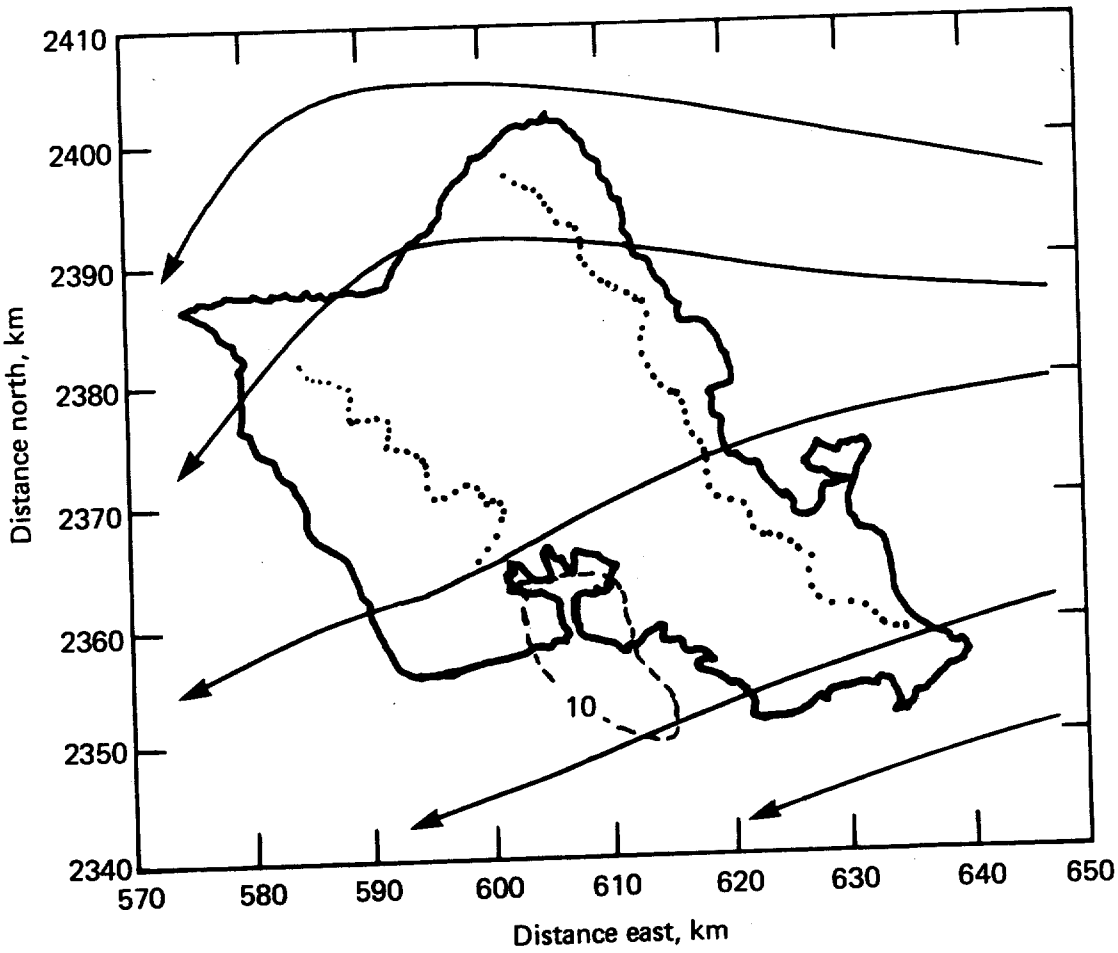

FIG. 6. Interpolated wind field 60 m above topography. The wind-speed isotach interval is 5 m/s.

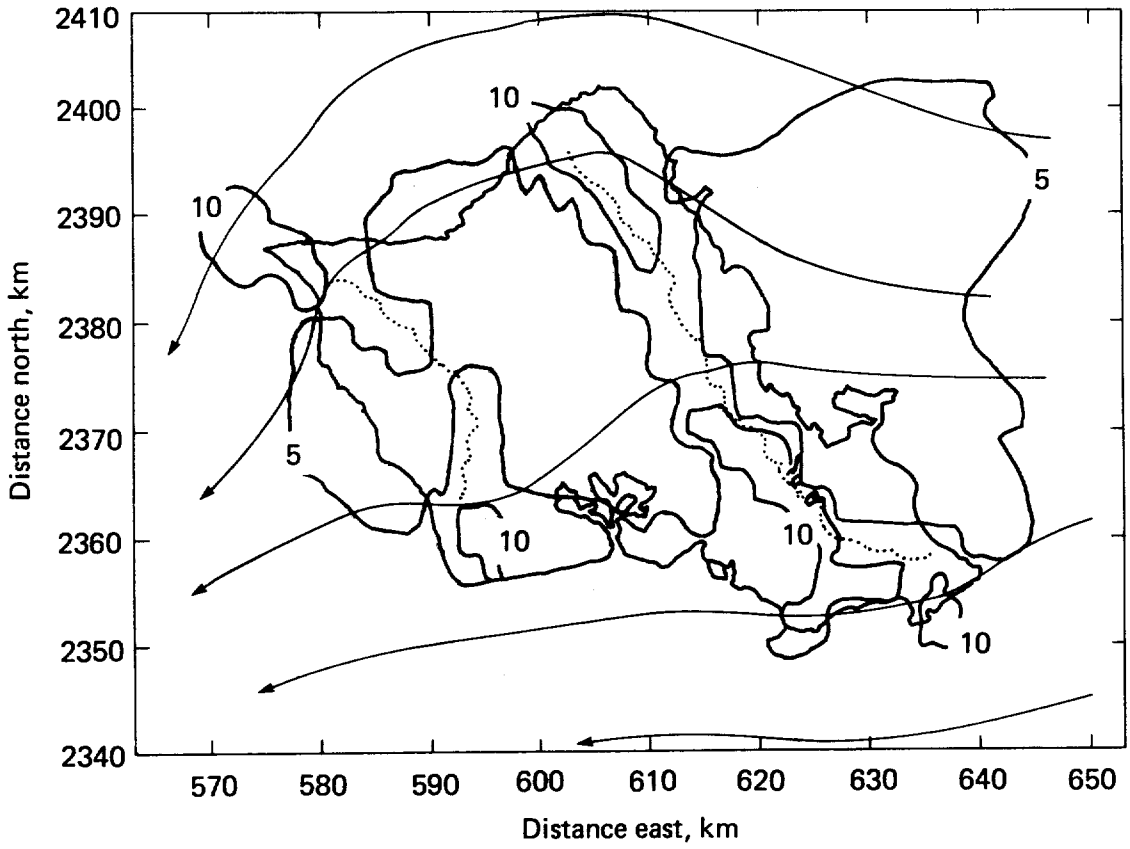

FIG. 7. MATHEW-adjusted wind field 60 m above topography. The wind-speed isotach interval is 5 m/s.

PRELIMINARY ASSESSMENT

Before a full data base is established, a preliminary identification of regions of potential wind enhancement is desirable. Since data will be very limited in this phase, the PCA pattern characterization step will be absent and only the MATHEW model will be used. The pattern analysis will be subjective and will be obtained by examining the historical record to find one or two patterns that describe the most commonly occurring flow fields. This is particularly easy for the island of Oahu because of the persistence of trade winds.

Multiyear historical records are available for nine stations on Oahu, many of which are no longer active. From a five-year set, we abstracted (Knox et al, 1976) the July wind data for 1400 LST and constructed a composite of the most frequent wind speed and direction for each station. These data, shown in Fig. 8, provided the input winds to MATHEW. Note that there is only one station in the northern part of the island, and this station is strongly affected by terrain.

Topographic contours of Oahu are shown in Fig. 9 at a contour interval of 100 m. These contours are based on the average elevation at a model resolution of 1.5 km in the horizontal. The digitized topography of Oahu, as resolved by MATHEW, is depicted in Fig. 10, where the vertical scale is greatly expanded to make terrain features more apparent. The view in Fig. 10 is from the southeast. The computational results appear in Fig. 11 as flow lines of the adjusted winds and isotachs of wind speed. The areas between contours have been shaded for added clarity. These maps show speed maxima on the corners of the island with minima in the central valley and immediately up and downwind to major topographic barriers. The significant wind maximum on the Kahuku hills was a striking early find because the northeast portion of the island was devoid of climatological measurements. This indicates the power of MATHEW as an early diagnostic tool in the siting study.

We used the wind-energy patterns from these prospector maps to help select four key wind-measurement stations. The rationale for siting these stations is as follows (See Fig. 1 and Table 1): the Laie station was positioned to document the tradewind flow off the ocean and on its approach to the natural airfoil of the Kahuku Hills; the Kahuku Hills station was located with good exposure in or near the indicated wind maximum in that subregion; the Waialua station was positioned to measure the wind speed and direction in the flow during its approach to Kaena Point; and the Mokuleia site was situated near one of several fine-structure wind maxima indicated in Kaena Point. By this means, we intended to acquire the highest quality data-base information for methodology testing.

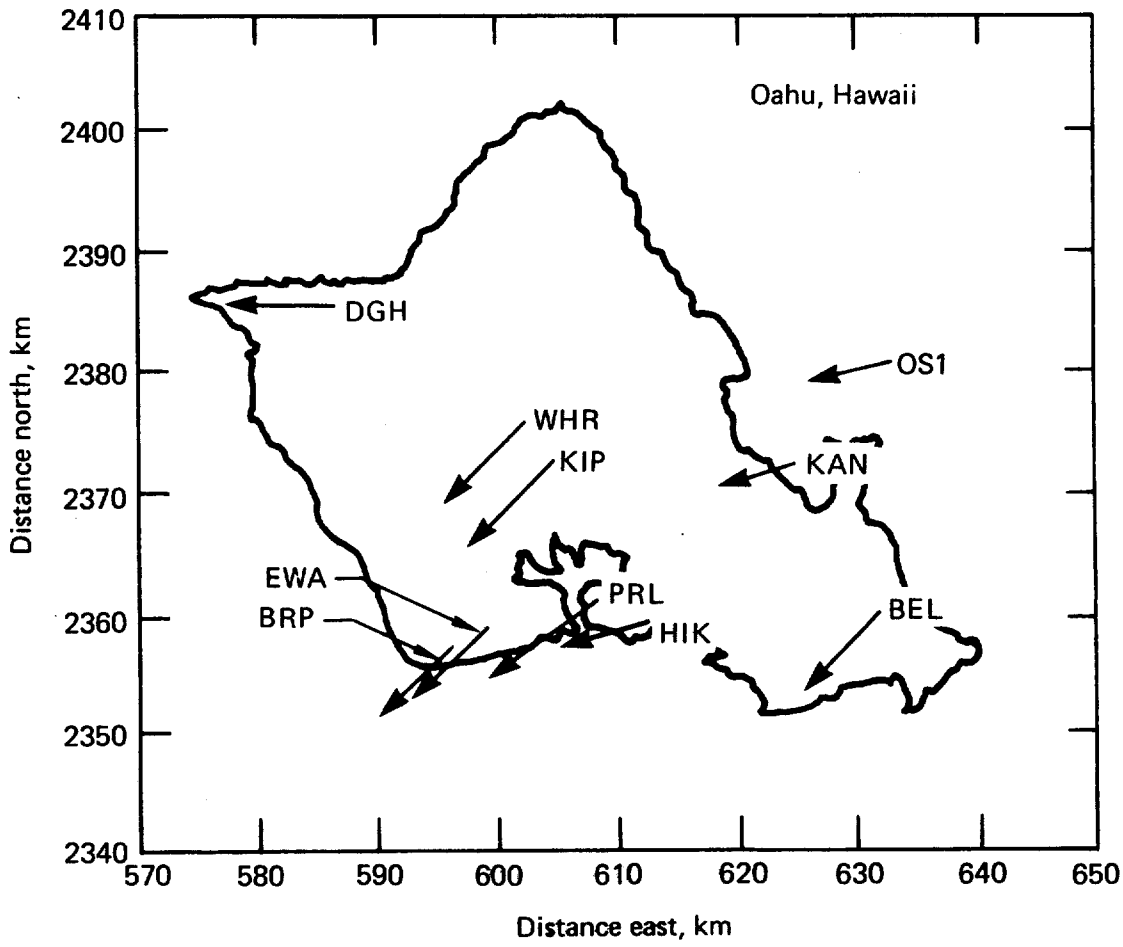

FIG. 8. Composite of the most frequent July wind speed and direction for 1400 LST abstracted from five years of historical records for Oahu, Hawaii.

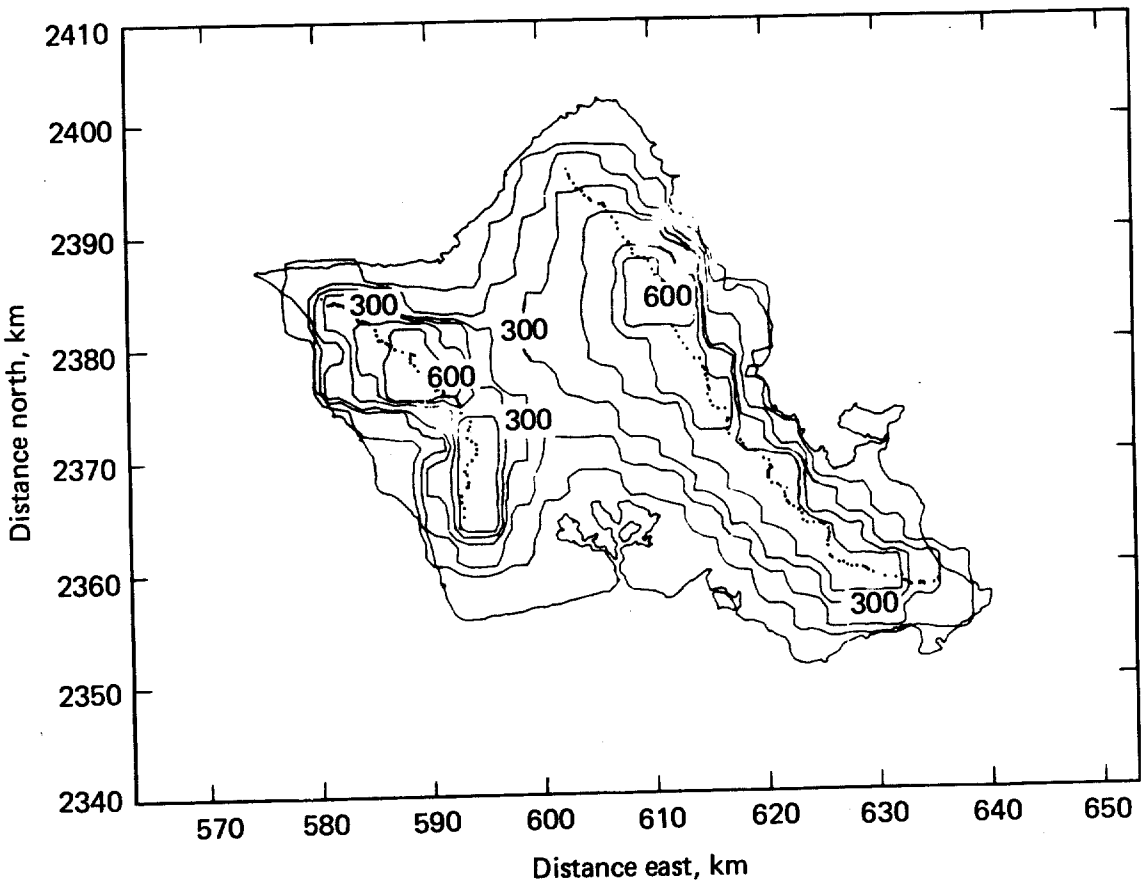

FIG. 9. Topographic contours for the island of Oahu, Hawaii, based on elevations averaged over 1.5 km. Contour interval is 100 m.

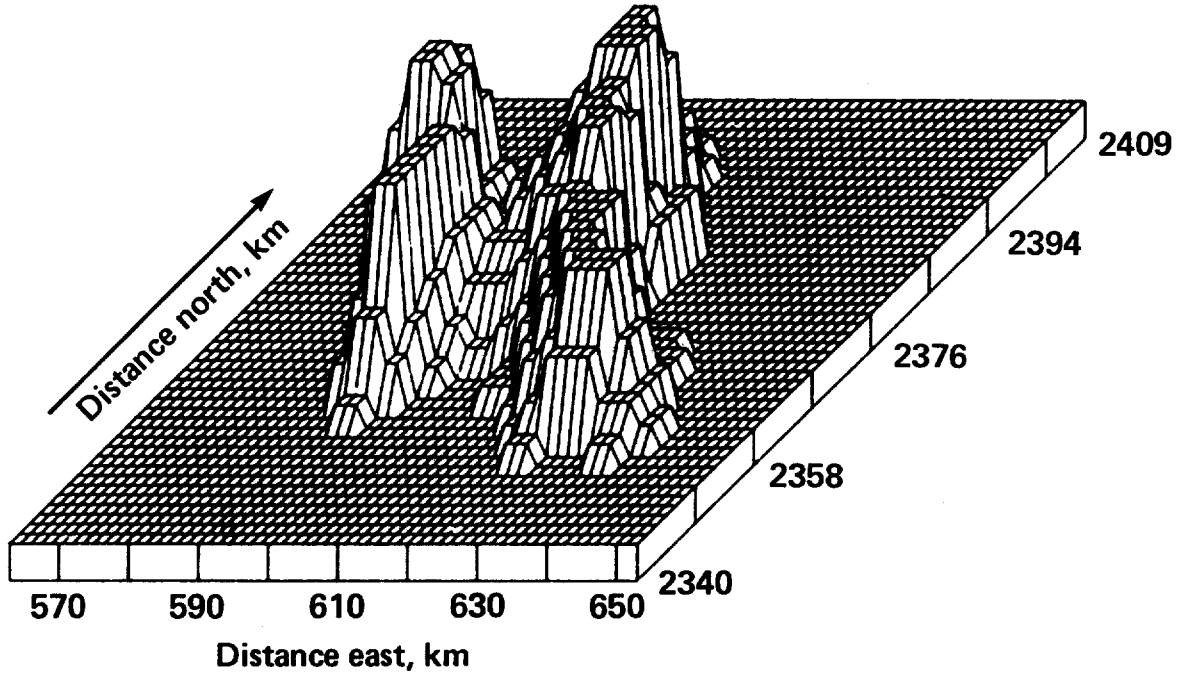

FIG. 10. Digitized topography of Oahu, Hawaii, viewed from the southeast. The vertical scale has been expanded to bring out terrain features.

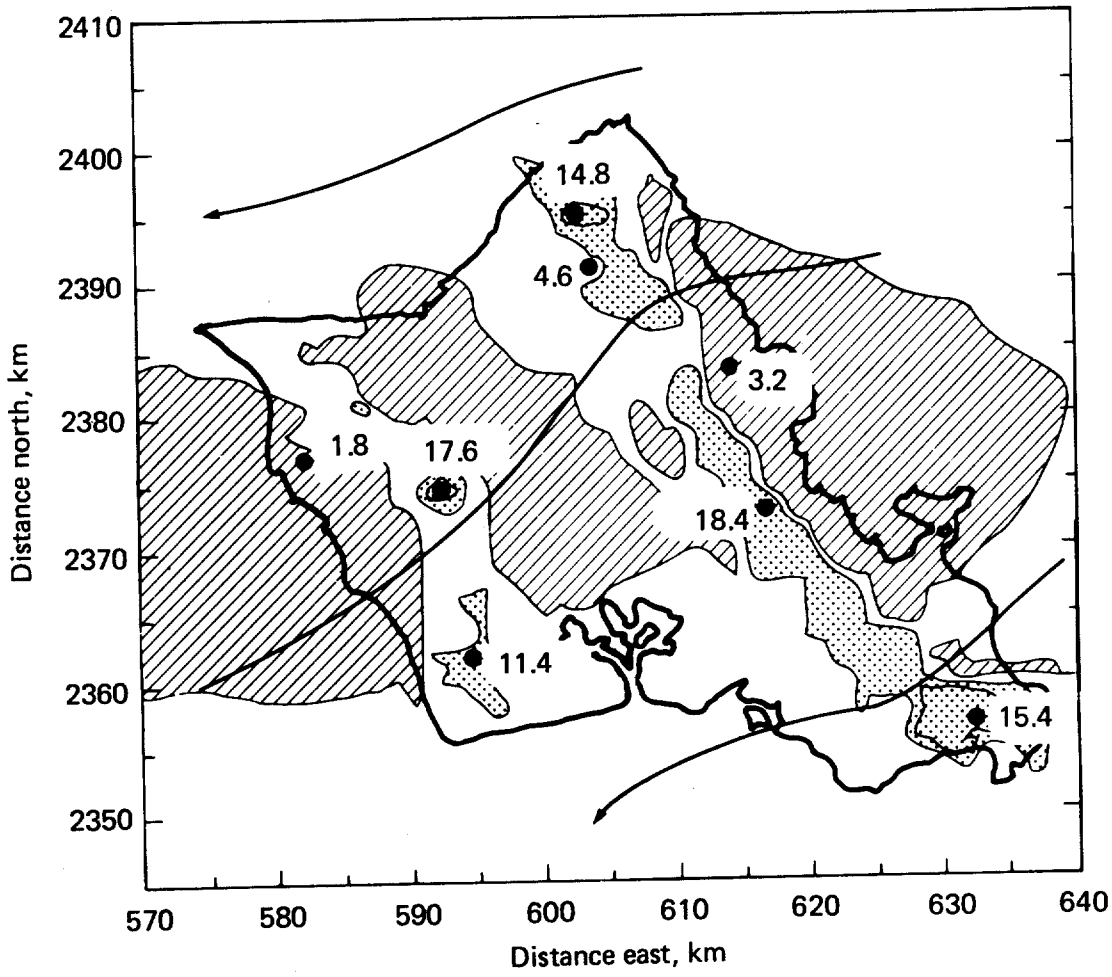

FIG. 11. MATHEW adjusted wind field 150 m above terrain for the composite 1400 LST July hour from historial data on Oahu, Hawaii.

DISCUSSION OF SITE-SCREENING PREMISES

We can now illustrate the site-screening premises, using the first year's data. Figures 12 - 14 show the effects of the various levels of data reduction that occur in the PCA/MATHEW screening process. For comparison, the duration curve obtained from the full data set is included in each figure. In all figures, the lines with squares were derived from the full data base, while those with circles were obtained from reduced data or predictions.

Two sites were considered:

Kahuku Hill and

Kaena Point (30 ft).

Both were identified as good potential wind-energy sites, and both provide an almost complete record for August 1976 - July 1977.

The first step in the screening process was to select typical days, using PCA. The data were analyzed by month, establishing groupings of similar days, their frequency of occurence, and that day of the month most representative of each group. This information appears in Table 2. All subgroups of days containing more than one day are also included. Table 2 is formatted by month and year, day best representing group 1 and, in parenthees, number of days represented. Succeeding columns contain the same information for other subgroups, if any. A dash in the day column indicates that, although a group with similar characteristics was identified, it was so vague that no day within the group was a good fit.

The second step was to run MATHEW for each day representing Group 1.* To save computation time, only every third hour of each day was run for this study. As will be discussed later, even eight samples per day is more than sufficient for adequate statistics. Once the calculations were completed the MATHEW predictions for each verification site were extracted for use in the subsequent analysis.

Figures 12a and 12b show that the subset of days selected by PCA is representative of the full year. The actual wind data from those days of each month that constitute the dominant spatial and temporal pattern were used to compute these duation curves. Comparison of these curves with those obtained from the full data set shows a fairly consistent set of high values. These high values of observed winds are a manifestation of the disproportionate influence strong wind conditions have on PCA. That is, the matrix used by PCA is based on unnormalized velocity products. Thus, correlated strong wind conditions will be reflected in this matrix and its eigenvectors when they are calculated.

*Because of the tradewind climatalogy of Oahu, a simple typical day sufficed to represent the regional flows each month. We would expect that wind sites for nontradewind sites more than one typical day per month could be required.

TABLE 2. Subgroups of days for August 1976 - July 1977.

Month	Group 1 Day	1 No.	2 Day	2 No.	3 Day	3 No.	4 Day	4 No.	5 Day	5 (No.)
1976										
August	2	(29)								
September	11	(25)								
October	13	(23)								
November	16	(21)	-	(2)						
December	6	(20)	4	(4)	30	(3)				
1977										
January	12	(23)	2	(2)	29	(2)				
February	6	(7)	-	(6)	5	(3)	-	(2)	22	(2)
March	18	(25)	-	(2)						
April	7	(19)	-	(5)						
May	7	(24)								
June	11	(21)	4	(3)						
July	11	(30)								

The effect of emphasizing strong wind conditions is also apparent when illustrating the second premise, which asserts that annual data may be represented by data from the typical days. Figures 13a and 13b are duration curves based on the weighted typical values for each month at the two sites. Each of these typical values is from the day of the month that is most like the PCA-generated average day. The actual annual statistics are again included for comparison.

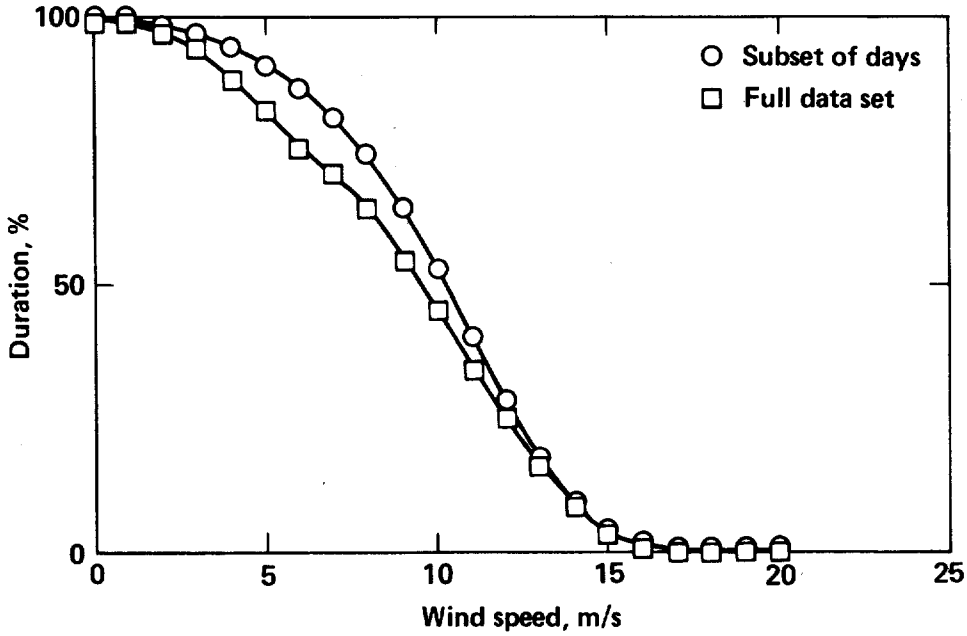

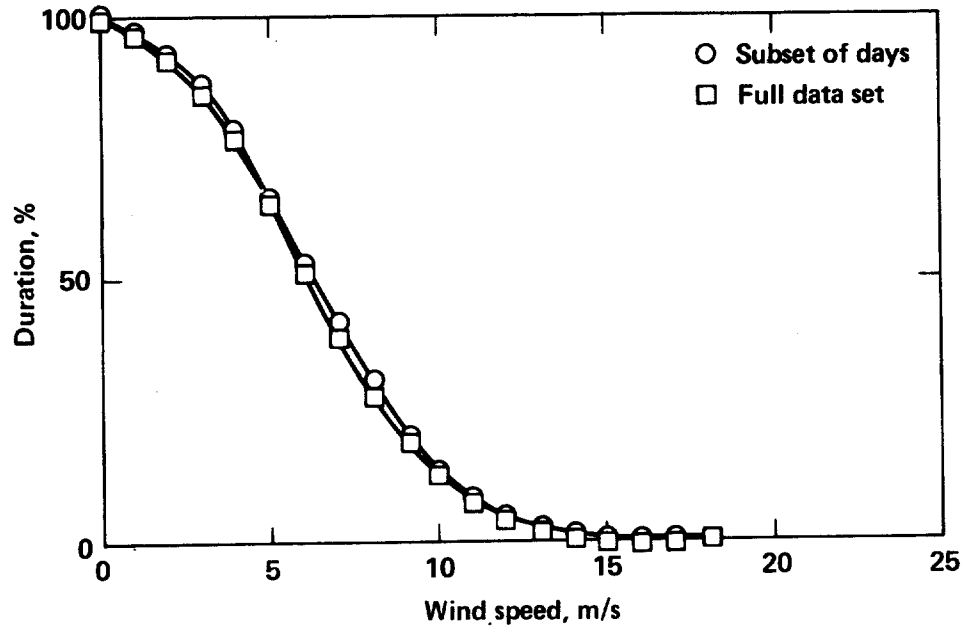

FIG. 12. Wind-speed duration curves at (a) Kahaku Hill and (b) Kaena Point (30 ft.) for August 1976 - July 1977 from The subset of days established using PCA and from the full data set.

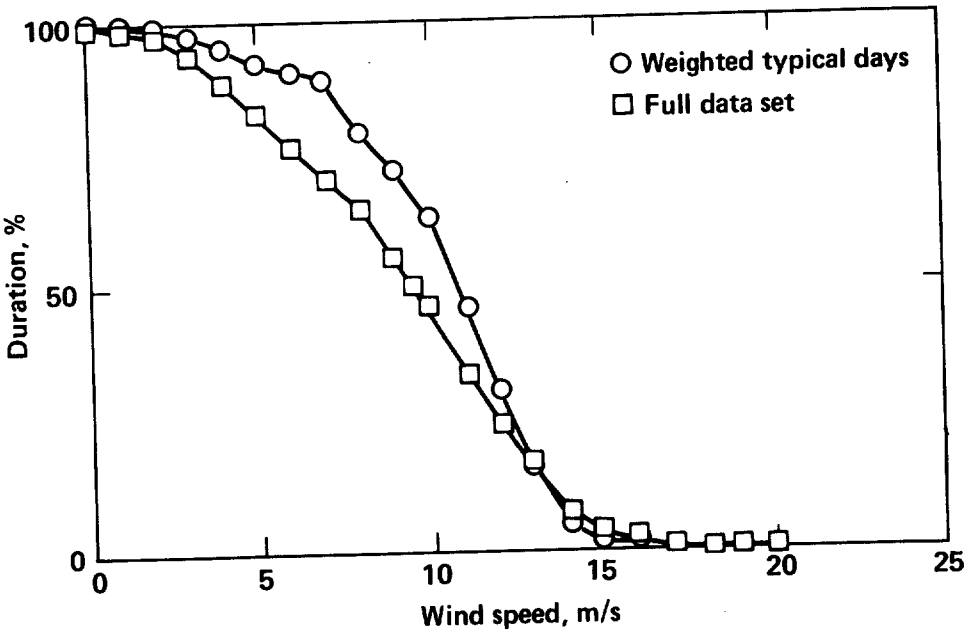

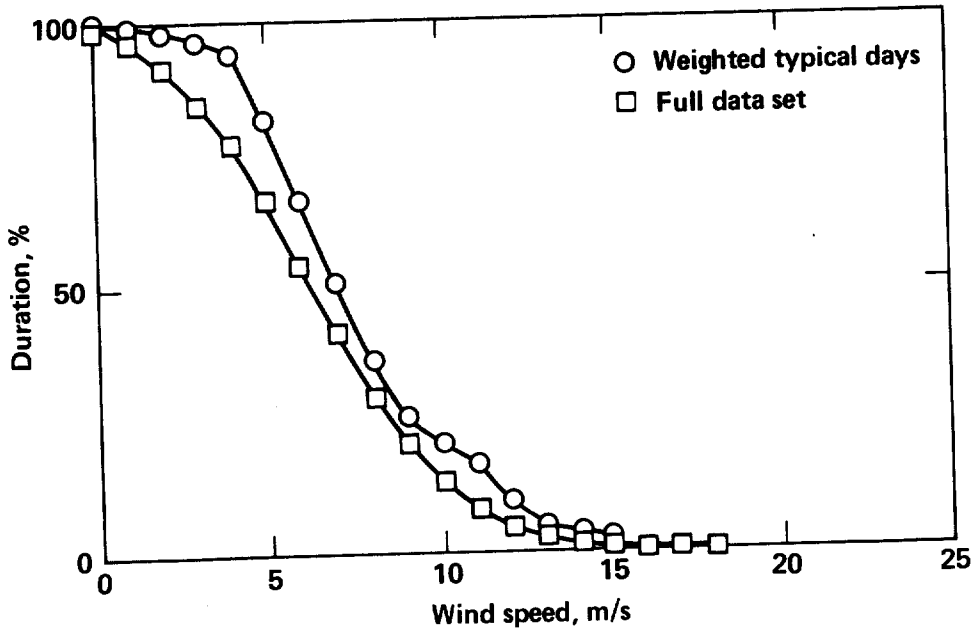

FIG. 13. Wind-speed duration curves at (a) Kahuku Hill and (b) Kaena Point (30 ft) for August 1976 - July 1977 from the weighted sums of typical days established using PCA and from the full data set.

Figures 14a and 14b illustrate the last of the three premises, namely that statistical information may be inferred at sites where data are not given. MATHEW was run on eight hours (2, 5, 8, and 11 a.m. and p.m.) of each typical day for each month. Data were not provided at Mokuleia, Maunawili, Honolulu Airport, Kaena Point (K3), Muana Kapu (MU), Koko Head, Kahuku Hill, and Tantalus so that the MATHEW predictions at these sites might be used for verification. In the figures, the duration curves produced from MATHEW predictions are compared with those from actual observations. The curves in Fig. 14a, for Kahuku Hill, show a clearly sharper dropoff at higher wind speeds. The comparatively poor agreement at Kahuku Hill, in contrast to that for Kaena Point (Fig. 14b), seems to be a result of the current version of MATHEW not reflecting the diversion of winds in the horizontal around topographic features. Preliminary results from a new version of MATHEW indicate that predicted horizontal components at this site become greater, as adjustments in the vertical component of the winds is constrained. More will be said about the new MATHEW later in this report. For the first year's analysis, at least, the Kaena Point 30 ft. tower observations are well represented by the weighted MATHEW predictions.

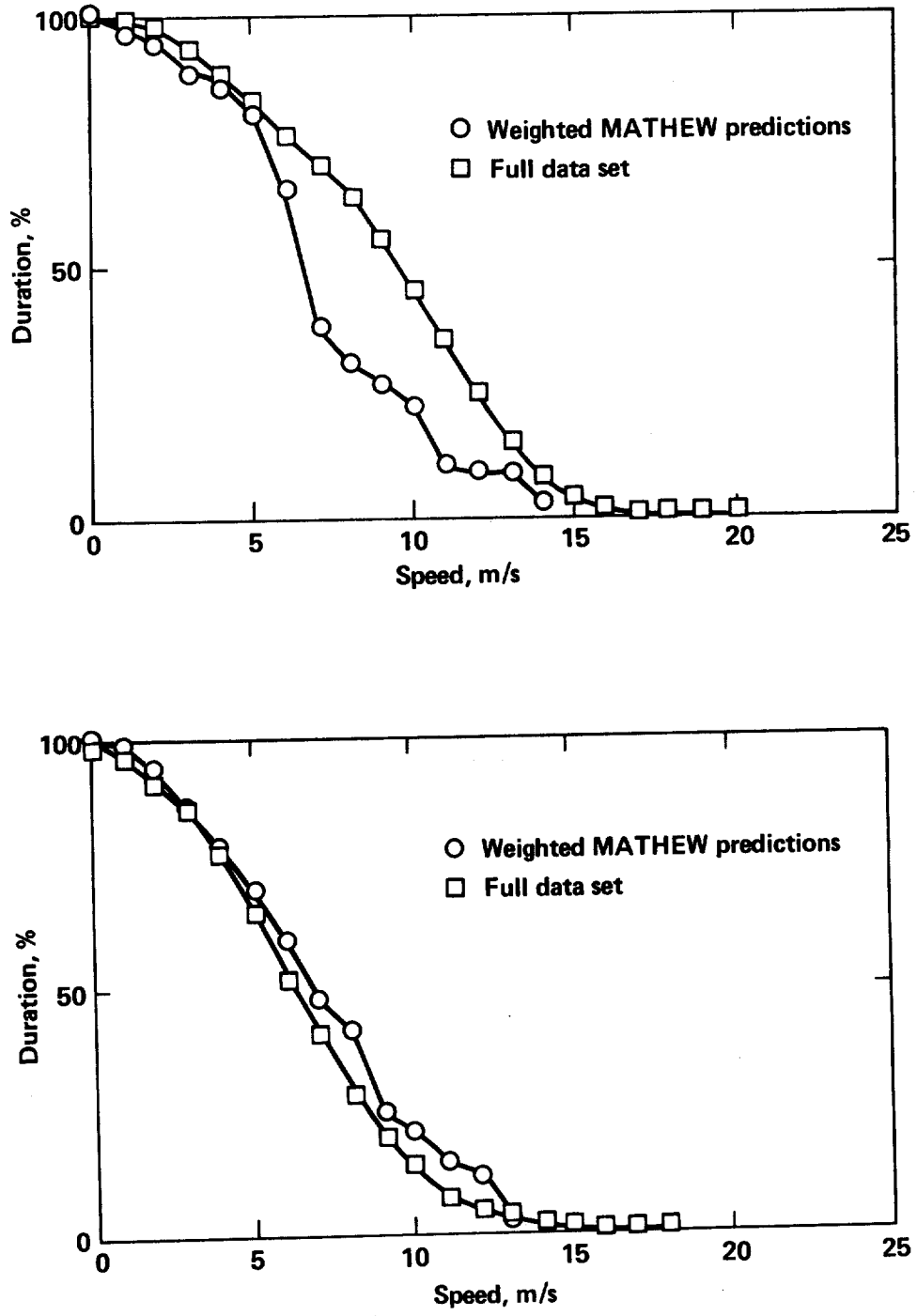

FIG. 14. Wind-speed duration curves at (a) Kahuku Hill and (b) Kaena Point (30 ft) for August 1976 - July 1977 from weighted sums of MATHEW predictions using PCA derived typical day inputs and from the full data set.

ANALYTIC FUNCTION FITS AND STATISTICS

From the preceding figures, we see that the PCA/MATHEW curves have wiggles and kinks not representative of the original data. Site-specific numbers (e.g., mean or median wind speeds) produced from such curves might give erroneous results because of shape deviations in portions of the curves. This leads us to the idea of an analytic function fit to the predicted curves from which pertinent wind characteristics could then be derived. Further, given an analytic function, other derived quantities may be readily computed. For example, given specific machine characteristics, we can compute the fraction of total available wind power that can be extracted by the machine. This can also be done with the actual data, but the analytic expressions make computation easier.

THE WEIBULL FUNCTION

The Weibull distribution (Justus, Hargraves, and Mikhail, 1976; Justus, Hargraves, and Yalcin, 1976) is an analytic function that has been found to fit the wind-speed duration curve data well and has been used in wind-energy analysis. The Weibull function is

$$W(s) = 100e^{-(s/c)^k} \quad , \tag{19}$$

where W is the percent of time the wind speed exceeds s. The parameters k and c are shape and speed factors, respectively. As k approaches 1, the curve begins to look like an exponential decay, if it is around 2, it looks like a Gaussian curve. The median wind speed, V_m, is related to the Weibull parameters by

$$V_m = c\,(\ln 2)^{1/k} \quad . \tag{20}$$

The average wind speed, V_b, is given by

$$V_b = c\,\Gamma\left(1 + \frac{1}{k}\right) \quad , \tag{21}$$

where Γ is the gamma function.

Figures 15 and 16 compare the Weibull fits from the MATHEW predictions with those from the full data base for the Kahuku Hill and Kaena Point (30 ft) sites. Note particularly the 20% low value of the c at the Kahuku Hill site. This will, of course, reflected in a low mean wind-speed prediction at this site.

The same calculations were also performed for the remaining verification stations (Auigust 1976 - July 1977): the Mokuleia Nike site, Honolulu Airport, Koko Head, Maunawili, Mauna Kapu, and Tantalus Tower. The various parameters were also computed in the same way for all verification sites, using data from the PCA-selected typical days, rather than MATHEW predictions. The results of these calculations are given in Table 3.

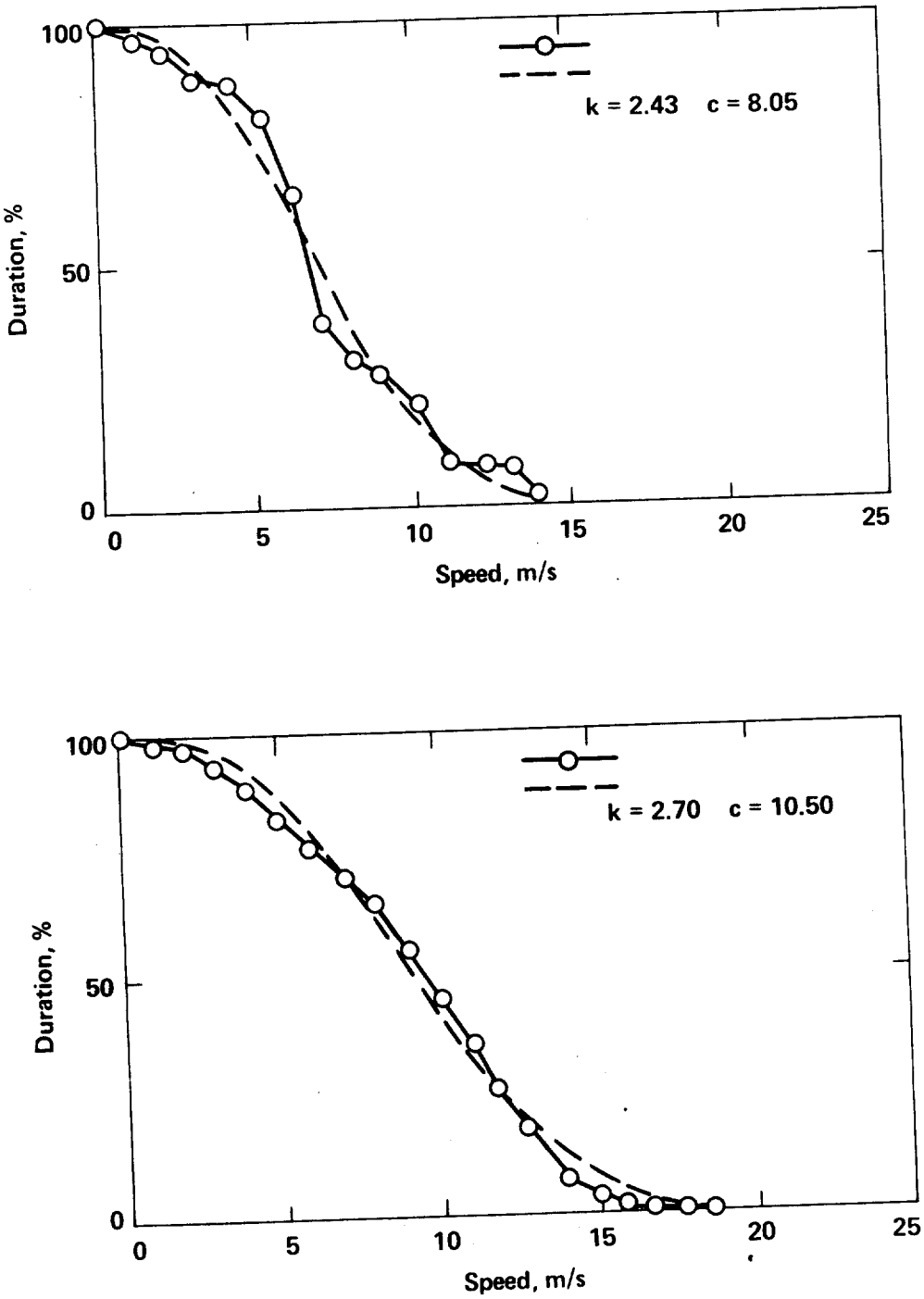

FIG. 15. Wind-speed duration curves at Kahuku Hill, obtained with (a) weighted MATHEW/PCA predictions and (b) the August 1976 - July 1977 data base and their Weibull fits.

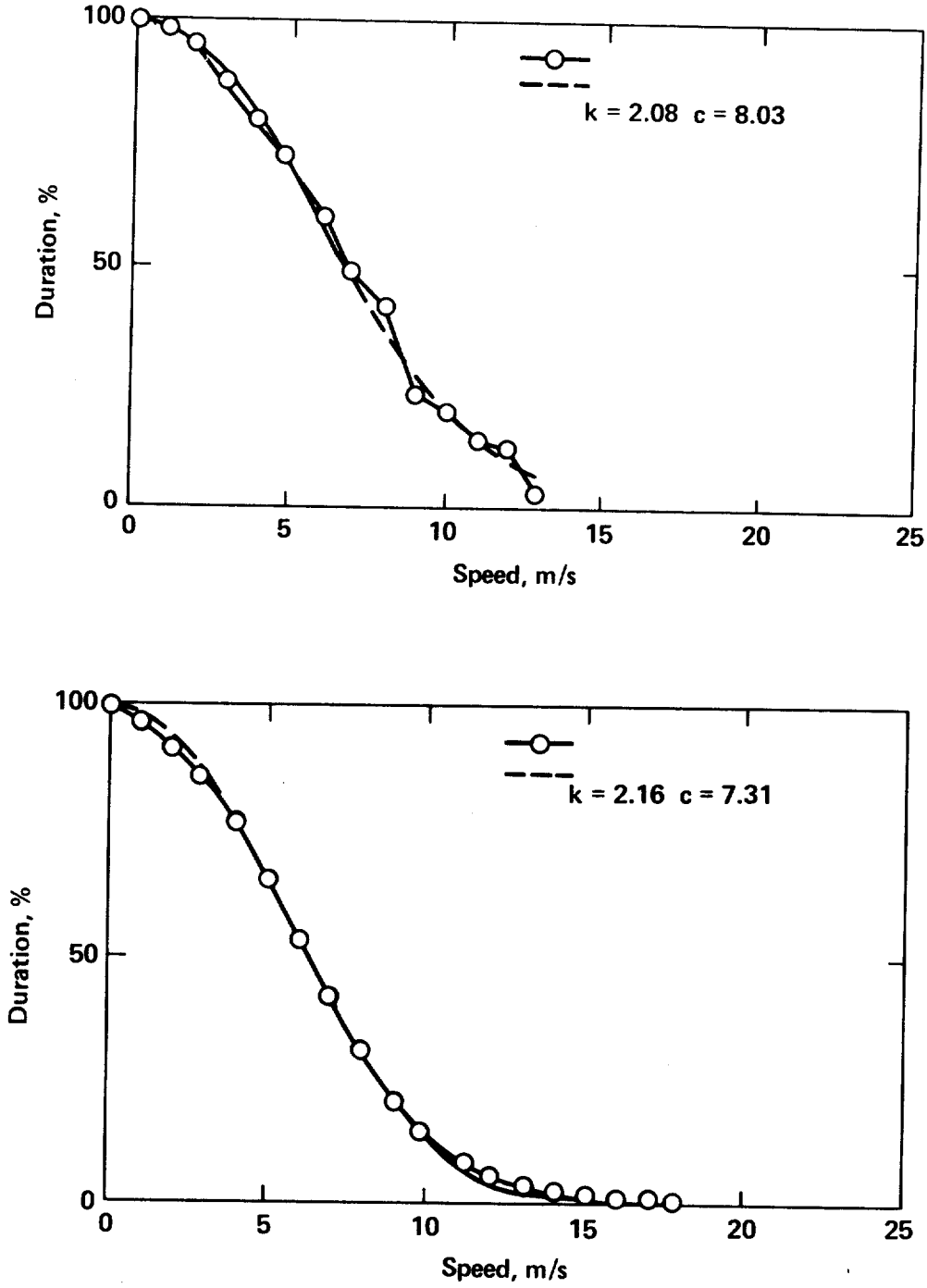

FIG. 16. Wind-speed duration curves at Kaena Point (30 ft.), obtained with (a) weighted MATHEW/PCA predictions and (b) the August 1976 - July 1977 data base and their Weibull fits.

TABLE 3 - The Weibill parameters k, c and mean wind speed V_b

ST[b]	K[a]			c[a]			V_b[a]		
	FD	WT	MP	FD	WT	MP	FD	WT	MP
MN	2.5	4.6	4.6	6.1	7.1	7.0	5.4	6.6	6.4
KH	2.7	4.5	2.4	10.5	11.5	8.1	9.3	10.6	7.1
HA	2.6	3.5	3.4	6.7	7.3	4.8	6.0	6.6	4.3
KK	2.7	3.2	3.3	10.7	10.8	6.7	9.5	9.6	6.0
MW	3.6	4.7	3.1	3.1	3.1	4.0	2.8	2.9	3.6
MU	2.0	2.9	3.0	8.3	9.8	7.2	7.3	8.6	6.4
TT	2.0	2.9	4.2	10.5	12.9	9.6	9.3	11.4	8.7
K3	2.2	2.7	2.1	7.3	8.3	8.0	6.5	7.3	7.1

a FD = from full data set, WT = from weighted typical days, and MP = from MATHEW predictions.

b Station symbol.

Scatter diagrams of these means are displayed in Figs. 17 and 18. In Fig. 17, the mean wind speed based on PCA-selected typical days is plotted against the mean speed based on the full data set. As indicated in the Objective Identification of Typical Wind Patterns section, we see that the PCA selection process tends to emphasize strong wind days. The worst sites are Mokuleia, Tantalus and Muana Kapu, where predictions are about 20% high. By contrast, Fig. 18, which gives the mean speed from the MATHEW predictions plotted against those from the full data set, shows more scatter on either side of the 45-degree line, corresponding to exact agreement. In fact, it shows a tendency to flatten out the predictions relative to the actual values.

These results reflect the effect on MATHEW predictions of the initial data-interpolation process. In this process, after all input data have been adjusted to a common height above terrain, a $1/r^2$ interpolation is made onto the computational grid. Now, consider a point at which terrain induced enhancement is expected but that is near data points that are in flat open areas. The interpolated field at this point will, of necessity, have the character of its nearest data points. In this case, the interpolated speed will be low. On the other hand, winds interpolated from ridge measurements down to flat open land will be too high. This phenomenon can be seen clearly in Fig. 19, in which we have plotted annual mean

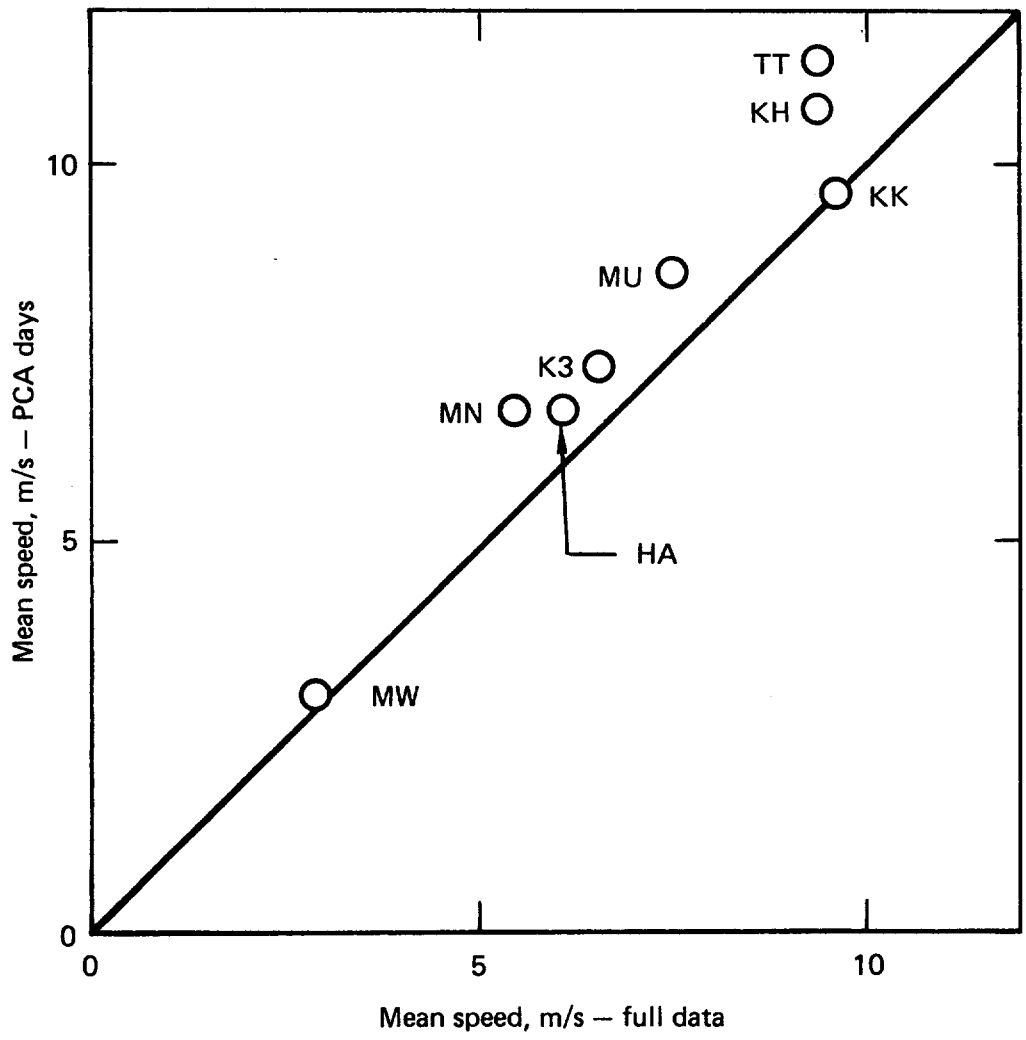

FIG. 17. Annual mean wind speed based on PCA-selected typical days plotted versus the mean wind speed based on the full August 1976 - July 1977 data set.

wind speeds computed from these initial interpolated fields versus those from the full data set. Since MATHEW does have limitations on the amount of adjustment it will do (minimal to achieve nondivergence), poor initial fields will taint the adjusted fields.

A comparison of the Figures 18 and 19 illustrates the benefit derived from the MATHEW adjustment of the wind field from the clearly defective initial interpolated wind field. The MATHEW adjustment, although restricted by the use of a minimal mass consistent alteration of the first guess, does provide a wind field that more nearly captures the observed terrain enhanced field shown in Figure 17.

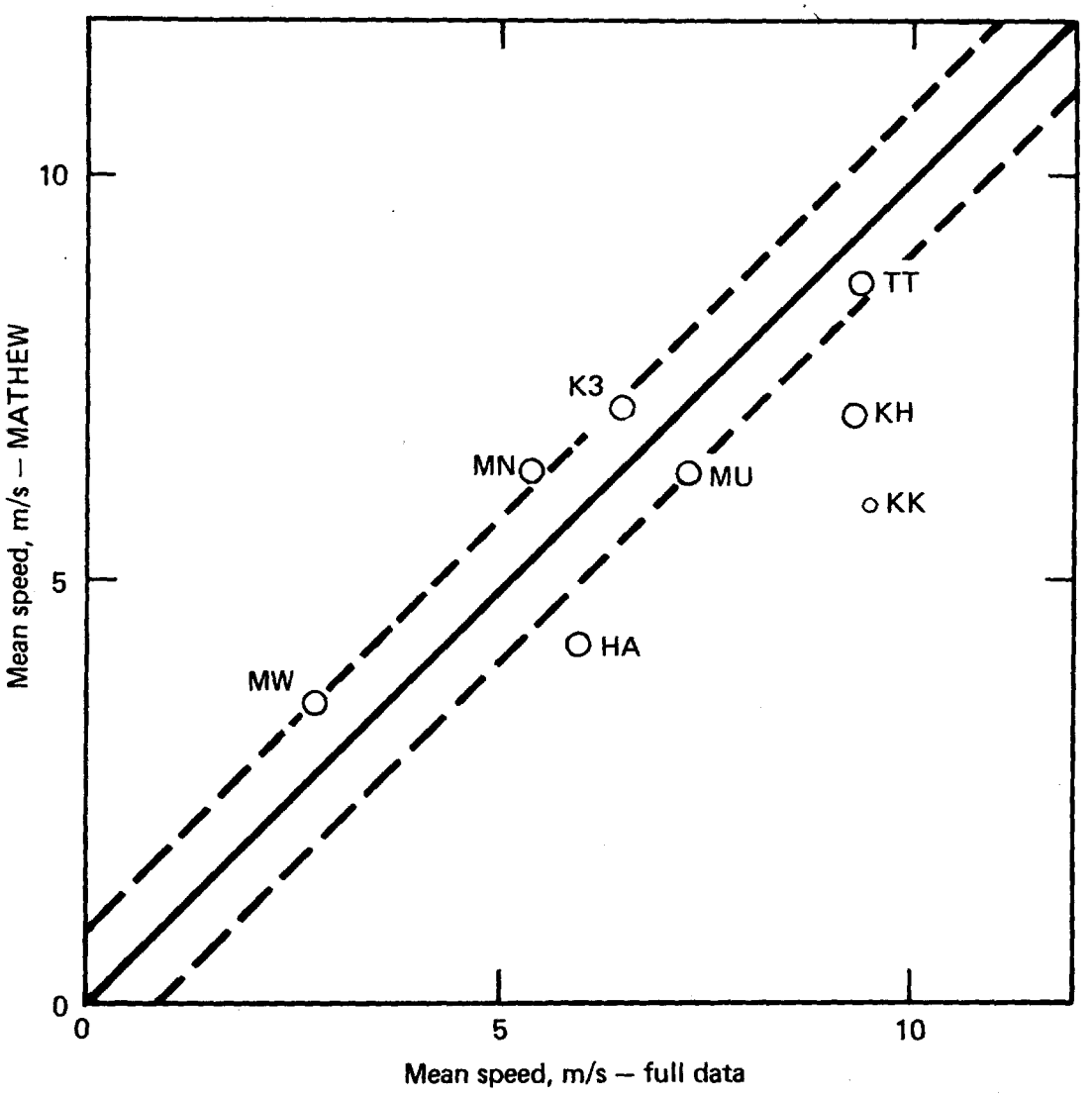

FIG. 18. Annual mean wind speed based on MATHEW/PCA-predicted winds plotted versus the mean speed based on the full August 1976 - July 1977 data set. The dashed lines define ± 1-m/s bounds.

A special comment must be made about MATHEW predictions at the Koko Head (KK) site. Data at this site are taken from an instrument 11 m above terrain that is 195 m above sea level. But Koko Head has small horizontal dimensions and is isolated from other topography. So, when the topography is averaged to go into MATHEW 's 1.5-km grid, Koko Head is reduced to sea level. For this reason, it is not seen as a point of wind enhancement. Reducing the horizontal grid scale and focusing on this site would produce enhancement. However, since Koko Head is comparatively small, it would not be considered a likely location for large-scale wind-power installations; therefore, a reduced-scale calculation for this area is not

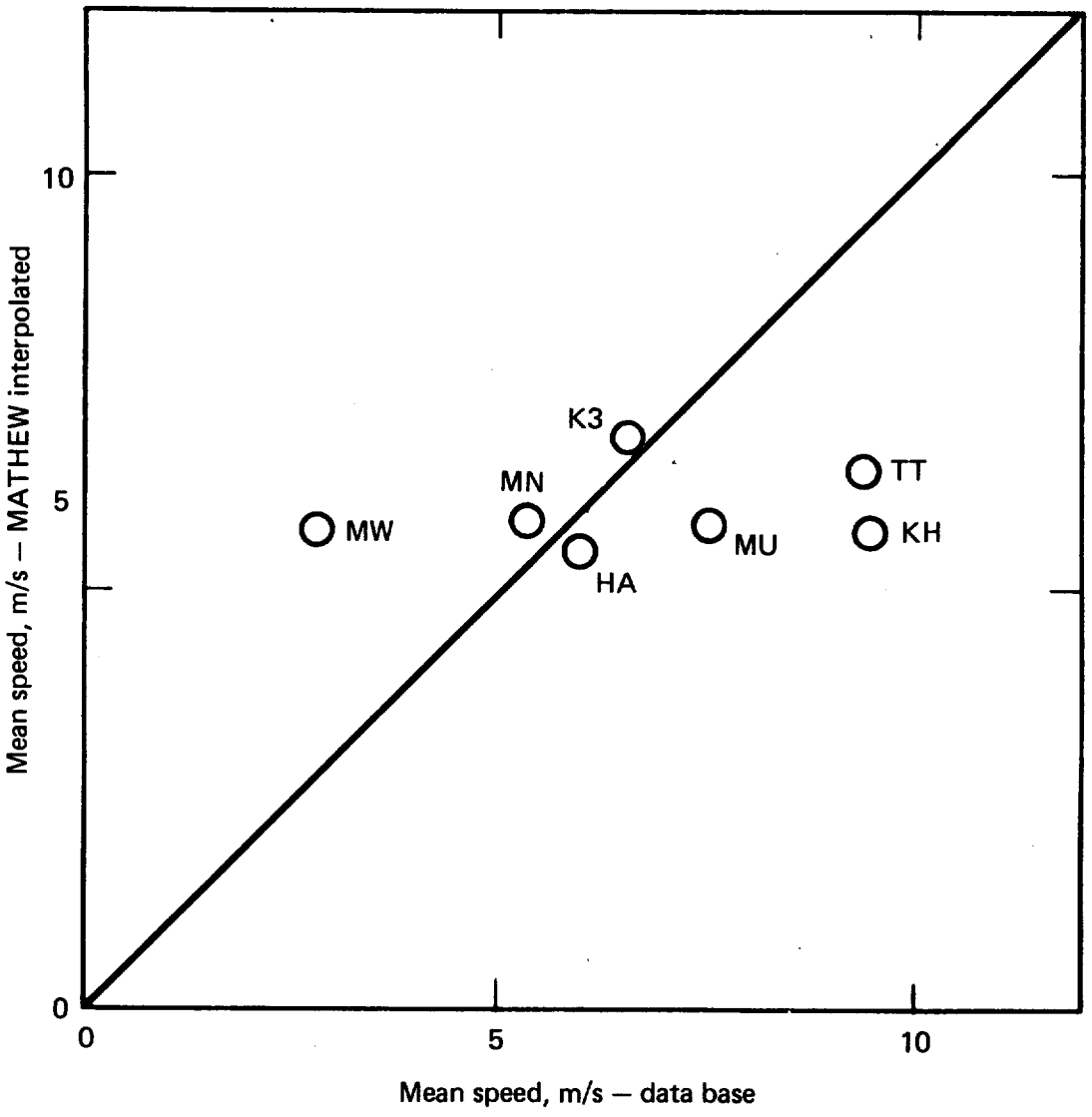

FIG. 19. Annual mean wind speed based on interpolated initial fields used by MATHEW versus mean wind speed from the full August 1976 - July 1977 data set.

warranted. The same argument should, in fact, be generalized to any small topographic feature. The only argument that can be made for such a scale reduction is the need for more detailed information about a specific site in order to locate wind-sensing instruments at the most favorable position within a sub-region.

Since Koko Head is small and does not reflect the large-scale wind enhancement we are looking for, it will not be included as a verification site in the remaining analysis. The question of its appropriateness as a data-input site will be addressed in the Regional Wind-Energy Potential section later in this report.

MEANS, MEDIANS—CURVES, WEIBULL FITS

In looking at the preceding curves, one might ask whether the use of means instead of medians is appropriate and whether the computation from a Weibull fit instead of the actual curves gives sufficiently accurate results. These questions can be answered in the affirmative by looking at the following table and scatter diagrams.

Table 4. gives the mean wind speed obtained, using the full data set and the MATHEW predictions, from the curves and the Weibull fit. The same type of information is included for the median wind speed.

TABLE 4 - Means/Medians - Curves/Weibull

	Means				Medians			
	Curves		Weibull		Curves		Weibull	
ST[a]	FD[b]	MP[c]	FD[d]	MP[e]	FD[f]	MP[g]	FD[h]	MP[i]
MN	5.4	6.5	5.4	6.4	5.4	6.5	5.3	6.5
KH	9.1	7.2	9.3	7.1	9.5	6.6	9.2	6.9
HA	5.9	4.3	6.0	4.3	6.0	4.3	5.8	4.3
MW	2.7	3.7	2.8	3.6	2.8	3.6	2.8	3.6
MU	7.2	6.4	7.3	6.4	7.1	6.3	6.9	6.4
TT	9.3	8.9	9.3	8.7	8.7	8.5	8.8	8.8
K3	6.4	7.0	6.5	7.1	6.2	6.8	6.2	6.7

[a]Station symbal.
[b]FD = Mean speed from the curves, using the full data set.
[c]MP = Mean speed from the curves, MATHEW.
[d]FD = Mean speed from the Weibull fit, full data.
[e]MP = Mean speed from the Weibull fit, MATHEW.
[f]FD = Median speed from the curves, full data.
[g]MP = Median speed from the curves, MATHEW.
[h]FD = Median speed from the Weibull fit, full data.
[i]MP = Median speed from the Weibull fit, MATHEW.

Figure 20 is based on the mean wind speed data in columns 2-5 of Table 4, and Fig. 21 shows the median wind speed data from columns 6-9 of Table 4. It is clear from these two plots that use of the mean or median, obtained from the actual curves or Weibull fits, will give virtually the same results. For the rest of this report, we have chosen to use mean speeds computed from the Weibull distribution.

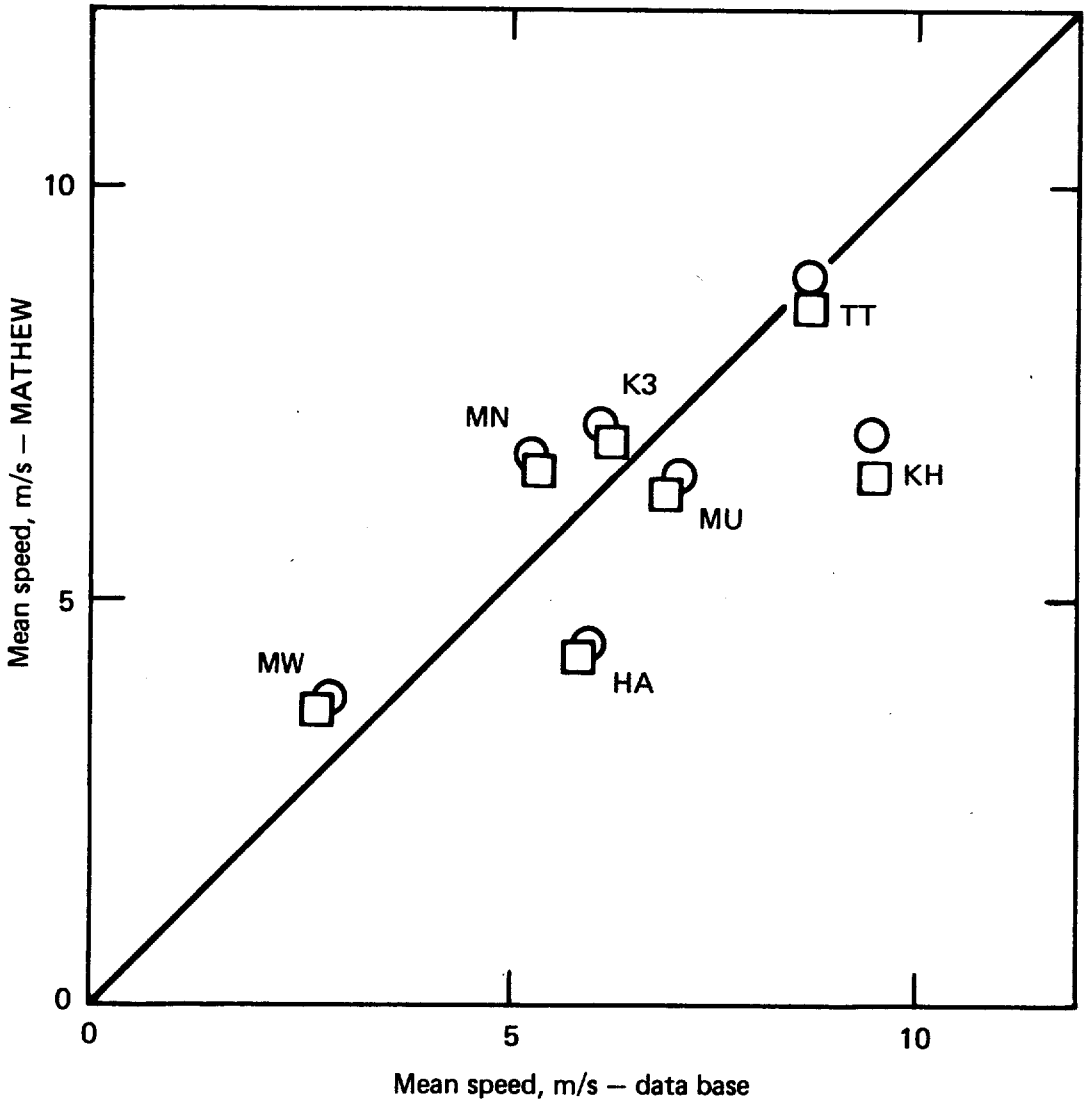

FIG. 20. Predicted annual mean wind speed versus that obtained from the full August 1976 - July 1977 data set from the MATHEW/PCA-generated wind-speed duration curve (circles) and from the Weibull fit to this curve (squares).

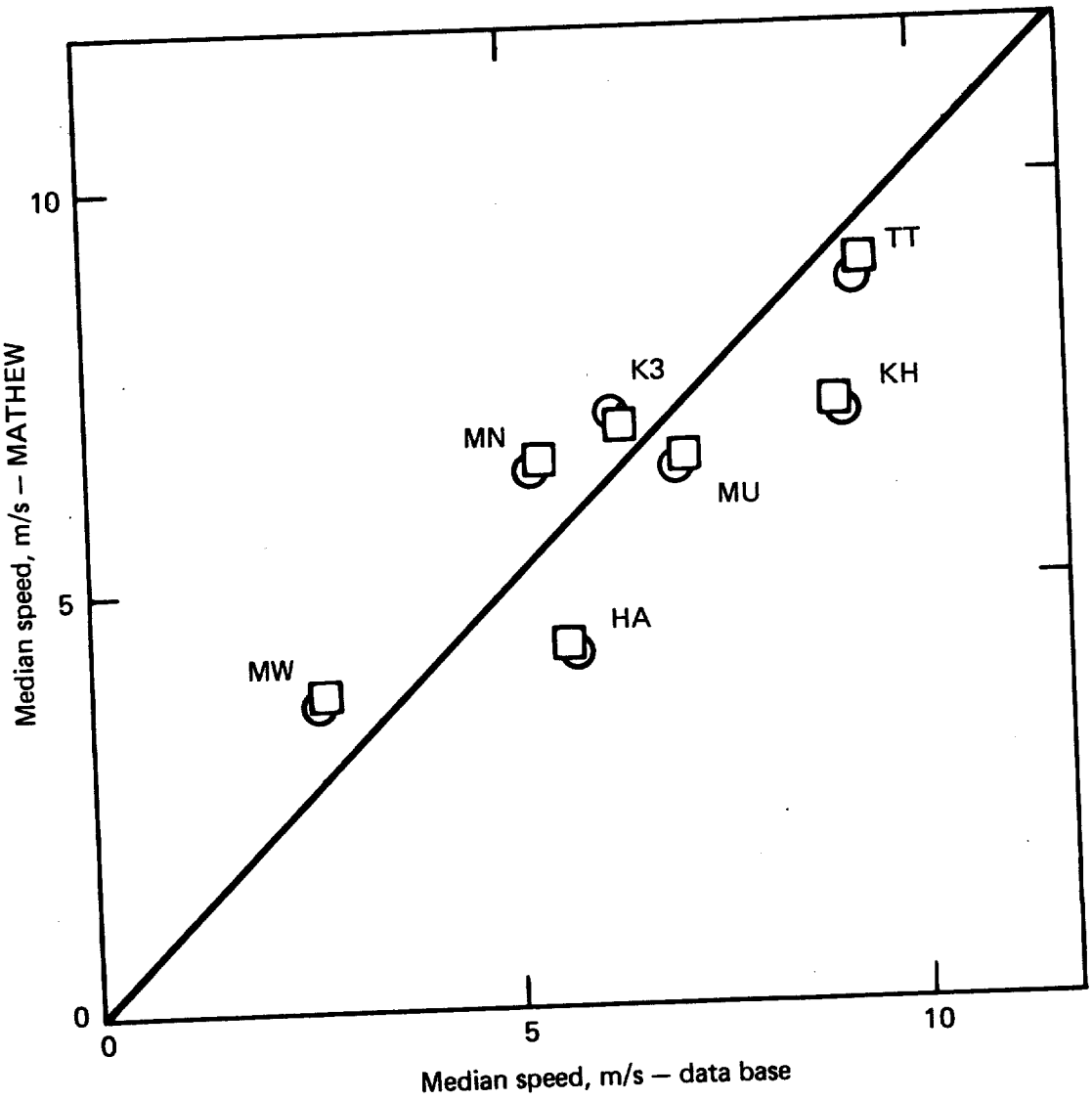

FIG. 21. Predicted annual median wind speed versus that obtained from the full August 1976 - July 1977 data set from the MATHEW/PCA-generated wind-speed duration curve (circles), and from the Weibull fit to this curve (squares).

REGIONAL WIND-ENERGY POTENTIAL

The site-specific wind-speed statistics we have described constitute one form in which site-screening data may be presented. In fact, they are the only form amenable to direct quantitative comparison with observation. We now go on to another form of data presentation, regional wind-energy potential.

The regional assessment is based on contours of wind-energy potential over the entire region at a specified height above terrain. MATHEW-predicted winds at a specified elevation and the PCA-determined frequency of occurence for each typical day are used to compute an annual mean V^3. Using the average air density, one can compute the average annual power. While the results do not lend themselves to direct verification, since data would be required for all points of the region, the resulting plots provide useful information on the location of sites of interest. This information is really a more-detailed version of the preliminary site-screening maps of wind speed over the region (Fig. 11).

Figure 22 shows contours of average annual power at 50 m for the island of Oahu for August 1976 - July 1970. Note the similarities between Fig. 22 and Fig. 11 from the preliminary analysis, particularly in the high ridgeline values and central valley low. Clearly, in a region where variations throughout the year were greater, this similarity between a single pattern and an annual average would not be as apparent. But, at the same time, the preliminary study in such an area would be made up of more than a single pattern and the detailed assessment would deal with a year divided, for example, into a season at a time.

The high wind-power areas are seen to follow the ridge lines on the eastern and western sides of the island. Enhancement is also indicated at exposed points of the island. Extension of the 200-W/m^2 contours off the computational domain is due to the fact that no data were provided at the boundaries. Therefore, the initial values that MATHEW adjusted were extrapolations from data on the island and did not reflect conditions offshore. We do not feel that reliance should be put on the specific location and magnitude of highs listed on Fig. 22 since they will be sensitive to the location of data sites and may be sensitive to such things as stability category, inversion height, and choice of the Gauss precision moduli. (Remember, it is the purpose of this analysis to identify regions of wind enhancement, not specific points.)

Normally, calculation and plotting of the regional power will precede the computation of wind statistics at specific sites because the regional power maps tell us where detailed wind-speed statistics will be most useful. One can envision circumstances in which the preliminary, climatological analysis might be obviated: for example, when there is already an extensive data base.

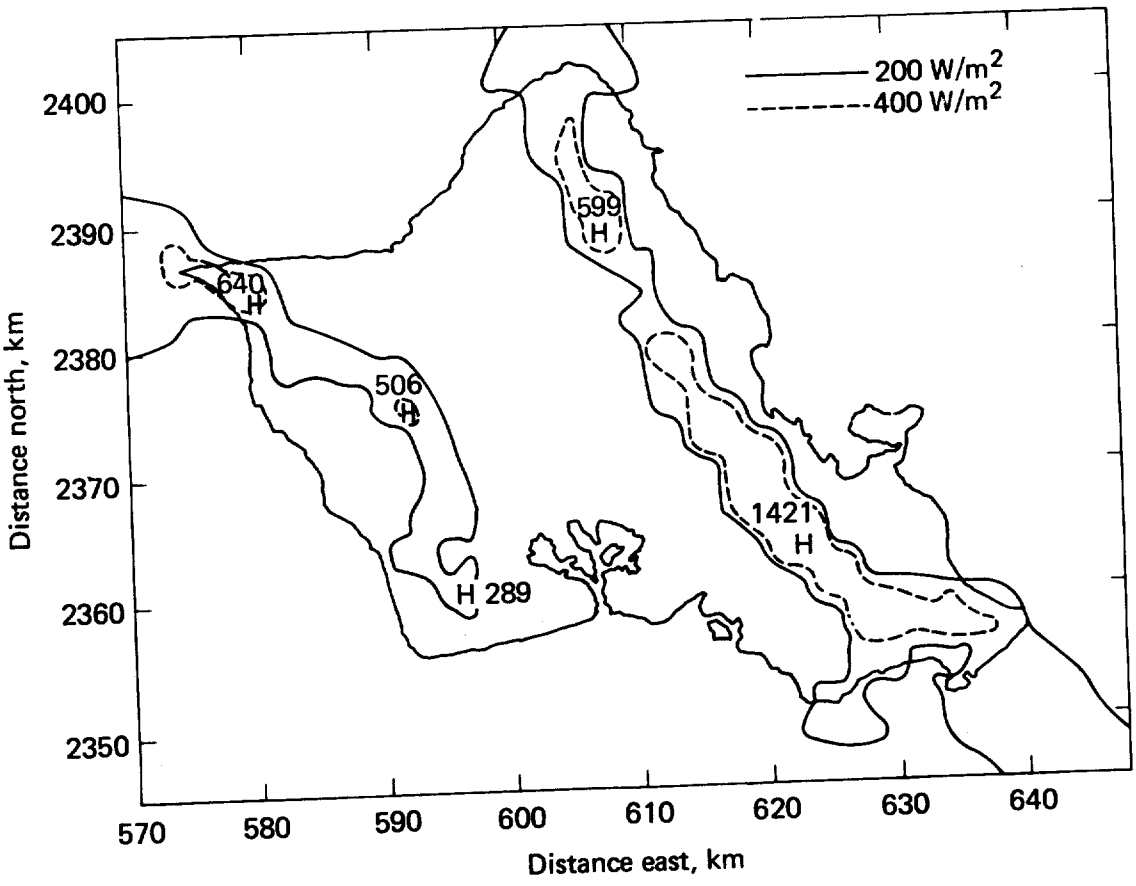

FIG. 22. Predicted annual average wind power at 50 m above terrain for Oahu, Hawaii for the period August 1976 - July 1977 based on MATHEW/PCA calculations. Contours are at 200 and 400 W/m^2.

SPECIAL CONSIDERATIONS

In the analysis and verification using the first year's data, we have learned about the amount of data that must be treated for meaningful statistics and how to locate sampling sites within the computational mesh in order to obtain best results. We will discuss these before going on to the second year's analysis.

REDUCING THE NUMBER OF DAILY SAMPLES

In the above analysis, all numbers based on MATHEW predictions used the results of 96 MATHEW runs, one every 3 hours of the typical day, starting at 2 a.m. for each of the 12 typical days. Yet, if we look at the primary eigenvector expansion coefficients for the typical day (see Fig. 4), we see little diurnal variation; the same is true for the other months analyzed. This leads us to believe that the number of MATHEW calculations required to perform the screening process may be reduced. We have, therefore, looked at the effect of using only two samples for each day; that is, instead of using hours 2, 5, 8, 11, 14, 17, 20, and 23, we might try hours 2 and 14 or 5 and 17, etc. The results of this experiment are shown in Figs. 23-26 for Kaena Point. Each figure represents 24 MATHEW runs and may be compared with Fig. 14b, which represents the results of all 96 runs. The results are not seriously degraded by the factor-of-4 decrease in calculations and are insensitive to the starting times. The same conclusion can be drawn for Kahuku Hill; see Figs. 27 and 14a for a comparison at this site.

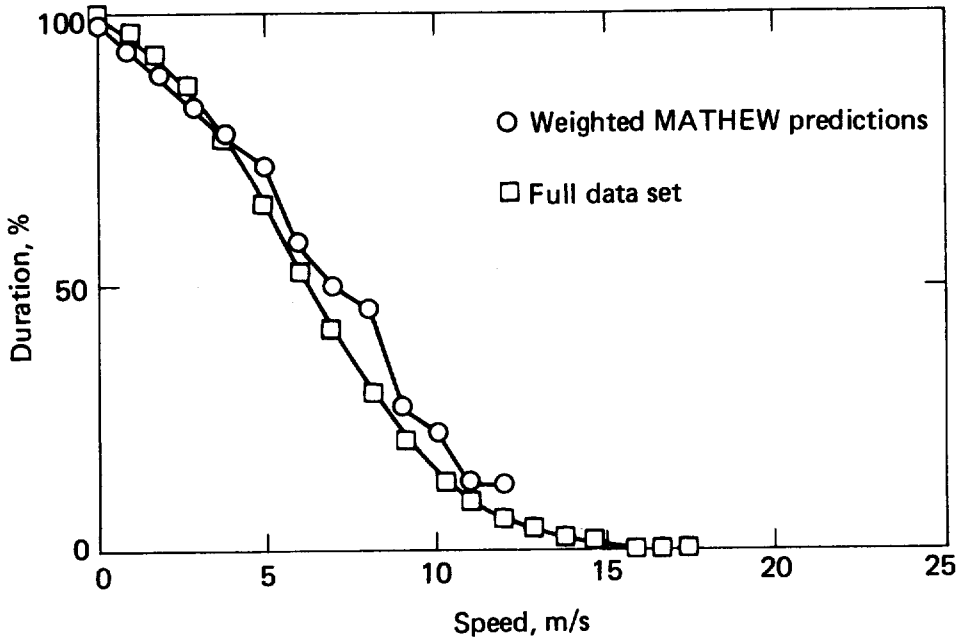

FIG. 23. Wind-speed duration curves at Kaena Point (30 ft.) for August 1976 - July 1977 from weighted MATHEW/PCA predictions at 2 a.m. and p.m. and from the full data set.

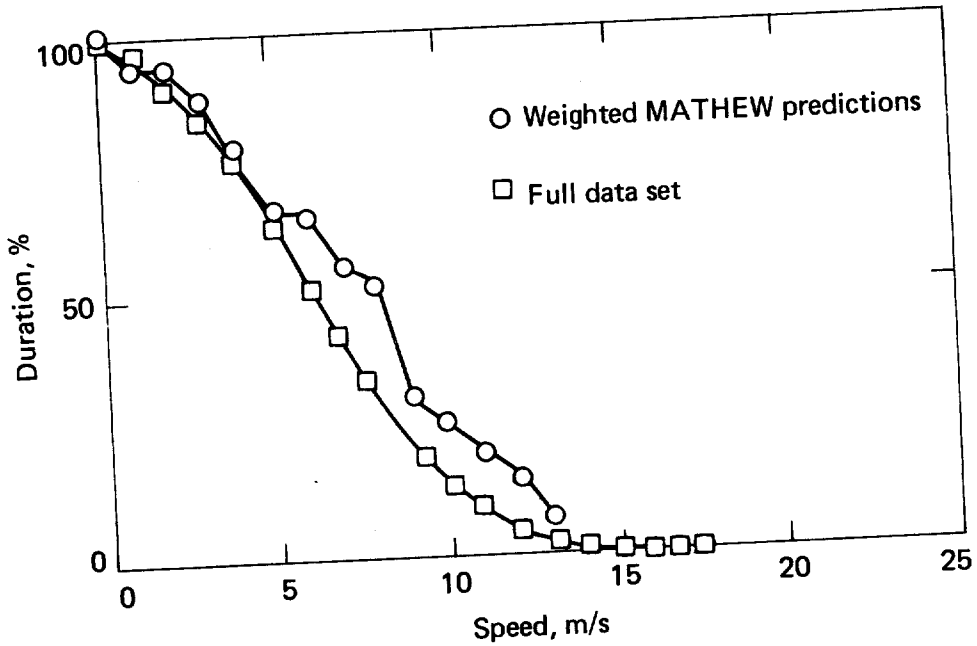

FIG. 24. Wind-speed duration curves at Kaena Point (30 ft.) for August 1976 - July 1977 from weighted MATHEW/PCA predictions at 5 a.m. and p.m. and from the full data set.

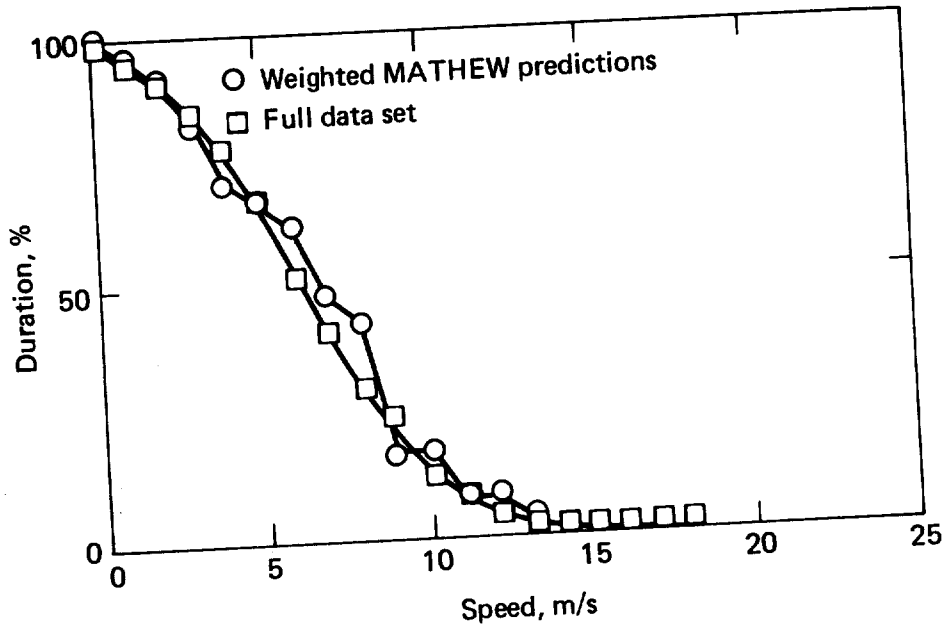

FIG. 25. Wind-speed duration curves at Kaena Point (30 ft.) for August 1976 - July 1977 from weighted MATHEW/PCA predictions at 8 a.m. and p.m. and from the full data set.

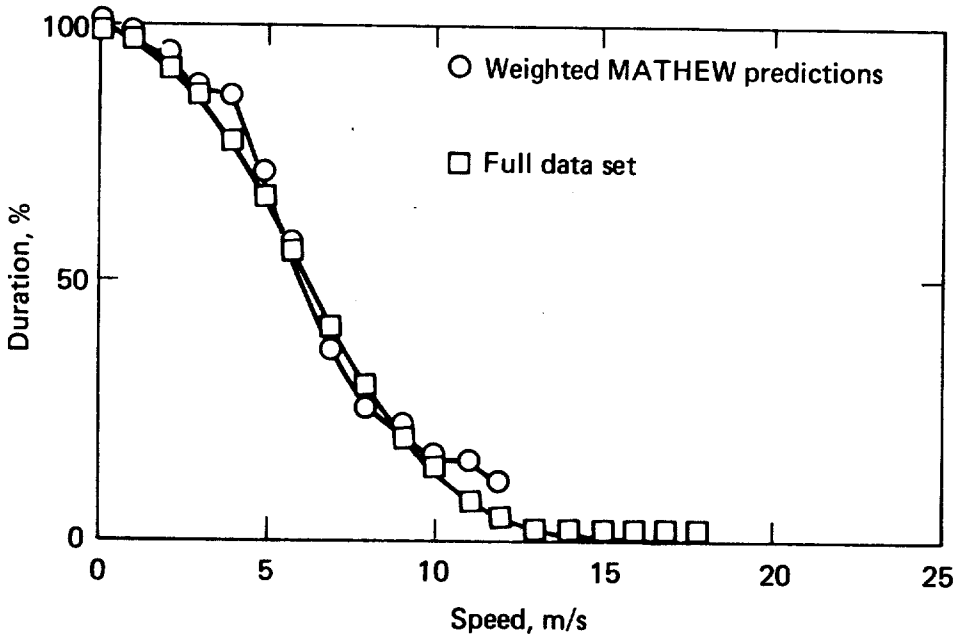

FIG. 26. Wind-speed duration curves at Kaena Point (30 ft.) for August 1976 - July 1977 from weighted MATHEW/PCA predictions at 11 a.m. and p.m. and from the full data set.

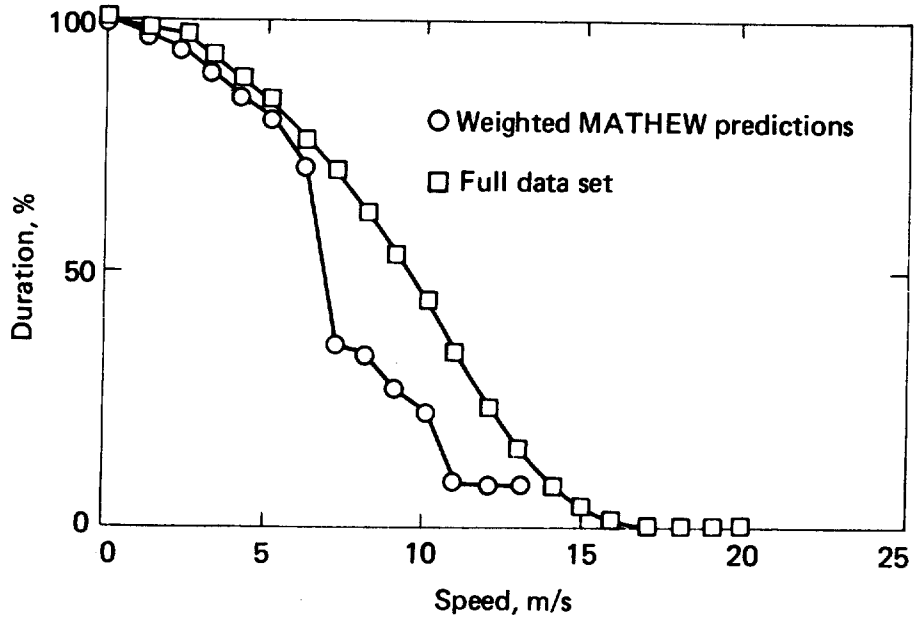

FIG. 27. Wind-speed duration curves at Kahuku Hill for August 1976 - July 1977 from weighted MATHEW/PCA predictions at 2 a.m. and p.m. and from the full data set.

Figure 28 further supports the assertion that the results with two samples per day are nearly as good as those for eight samples per day. In this figure, the mean wind speed based on Weibull fits to MATHEW predictions for 2 a.m. and 2 p.m. is plotted against means from the full data set. If Fig. 28 is compared with Fig. 18, the results are effectively the same; yet Fig. 28 represents only 25% of the computation time required to produce Fig. 18.

On the basis of the above results, we have decided to produce statistics from only two data samples per day in the remainder of this report. The sample times will be 2 a.m. and 2 p.m. of each typical day. Again, this reduction will be realized only in areas that have particularly simple diurnal behavior, like that observed on the island of Oahu.

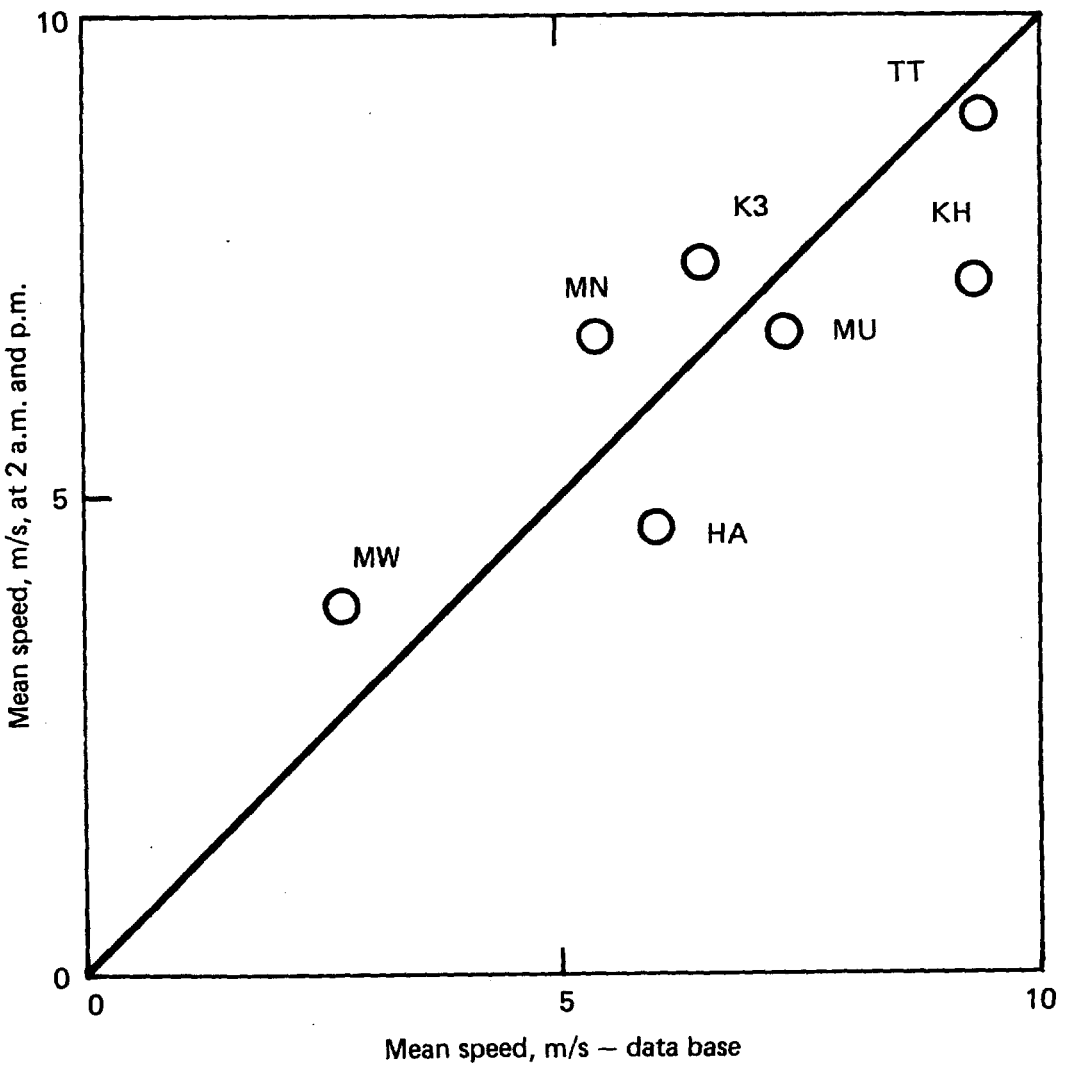

FIG. 28. Annual mean wind speed based on MATHEW/PCA predictions at 2 a.m. and p.m. versus that obtained from the full data set.

EFFECT OF USING MORE THAN ONE TYPICAL DAY

The original idea for obtaining one year of statistics from MATHEW, derived from PCA-produced days, was to use a day that represented each type of day identified. Suppose, for a given month, that a primary pattern were representative of 20 days, that a secondary pattern were representative of 8 days, and that 3 days looked like no other day, then 5 types of days would be run through MATHEW and the results would be summed with weightings of 20, 8, 1, 1, and 1. Clearly, if we are rigorous enough in defining similar days, this subset will provide a very good statistical representation of the full data set.

To reduce the amount of computer time used in the MATHEW computations, we have chosen instead to run only the most frequent pattern. This pattern, for the reasons mentioned earlier, can be expected to emphasize days with stronger winds, as is reflected in Fig. 17. To look at the effect of including additional types of days in the analysis, we have generated statistics and a scatter plot of mean wind speed, Fig. 29, for months having two characteristic patterns. This figure shows the mean speed as squares using one day per month vs that using all data (this is just Fig. 17 again), and as circles, the mean wind speed using two days per month vs that using all data.

Inclusion of the second pattern decreased the predicted mean by about 4%, bringing it closer to the actual value. If the criteria for similarity were made more stringent and more days were used for the statistics, the results would be improved; however, the improvement is not considered worth the added computational expense. The same kind of argument has been already made for using only two hours to represent a day, rather than four, eight, or more hours. In an area having more complex diurnal behavior, more hours per day will be required. The user will readily see from the PCA output whether more than one typical day or more hours per day will be required to produce useful statistics.

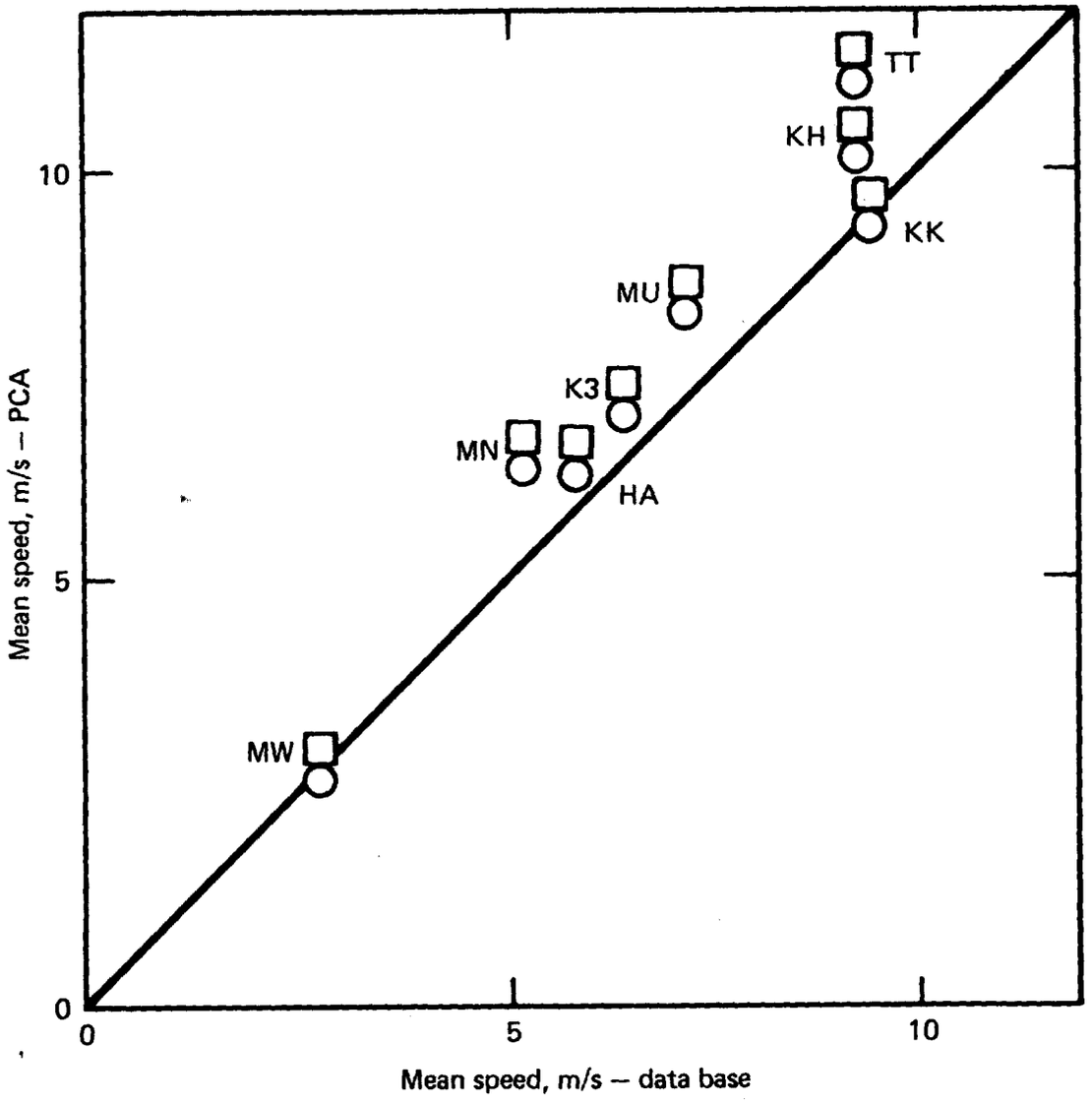

FIG. 29. Predicted annual mean wind speed using one PCA-established typical day per month squares and two PCA-established typical days per month circles, versus that obtained from the full data set.

SITE LOCATIONS WITHIN THE MATHEW-AVERAGED TOPOGRAPHY

Figure 10 shows that averaging, performed on the topography to provide a lower boundary for MATHEW, produces a very blocky surface. What is not as apparent is the effect this averaging can have on the predicted winds at specific sites. This problem is illustrated in Figs. 30a and 30b, which show the same topographic feature averaged from slightly shifted origins. In Fig. 30a, the site (*) is shielded by terrain from winds blowing right to left and by a blockage when the winds blow from left to right. In Fig. 30b, on the other hand, the site is located on elevated terrain and is more likely to be subject to enhanced winds.

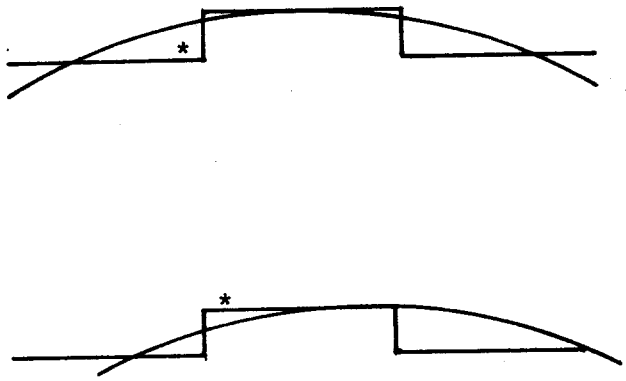

FIG. 30. (a) Averaged topography for an elevated area, and (b) with the origin for averaging shifted one-fourth of a zone.

For this reason, care must be exercised in placing of sites in the MATHEW topography. Rather than put the site at precisely the location given by its UTM coordinates, it must be put at that point within the MATHEW topography that is both closest to its UTM coordinates and still representive of its surrounding topography.

In our calculations, three sites were shifted: Tantalus Tower was shifted 1.5 km to the east, Maunawili was shifted 0.5 km to the northeast and, for the second year's calculations, Comsat was shifted 1.5 km to the east. While the shift of Comsat did not significantly improve the results, that for Tantalus was quite dramatic; here the shift was equivalent to that shown in Figs. 30a and 30b. Tantalus is exposed to winds from the east but, when placed at the coordinates given in Table 1, was sheltered as shown in Fig. 30a. Figure 31 is a plot of the annual wind-speed duration curve obtained at this location, where the mean wind speed was calculated to be 4.3 m/s. Figure 32 is the duration curve obtained for a site located on the elevation, as shown in Fig. 30b. For this site, the mean wind speed is 8.7 m/s.

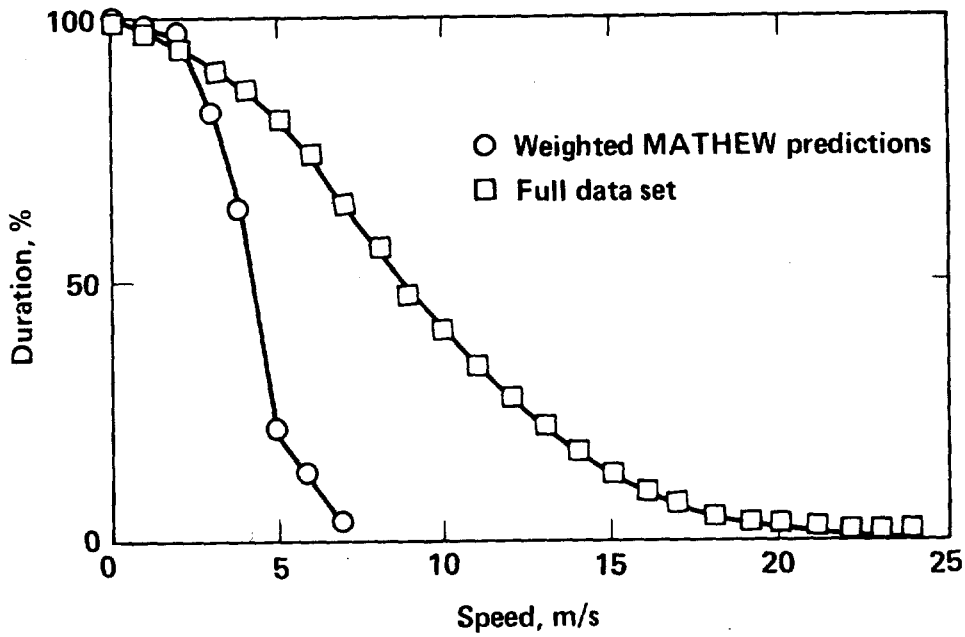

FIG. 31. Wind-speed duration curve from MATHEW/PCA predictions for the Tantalus Tower site, improperly located in the terrain (circles), and the duration curve from the full data set squares.

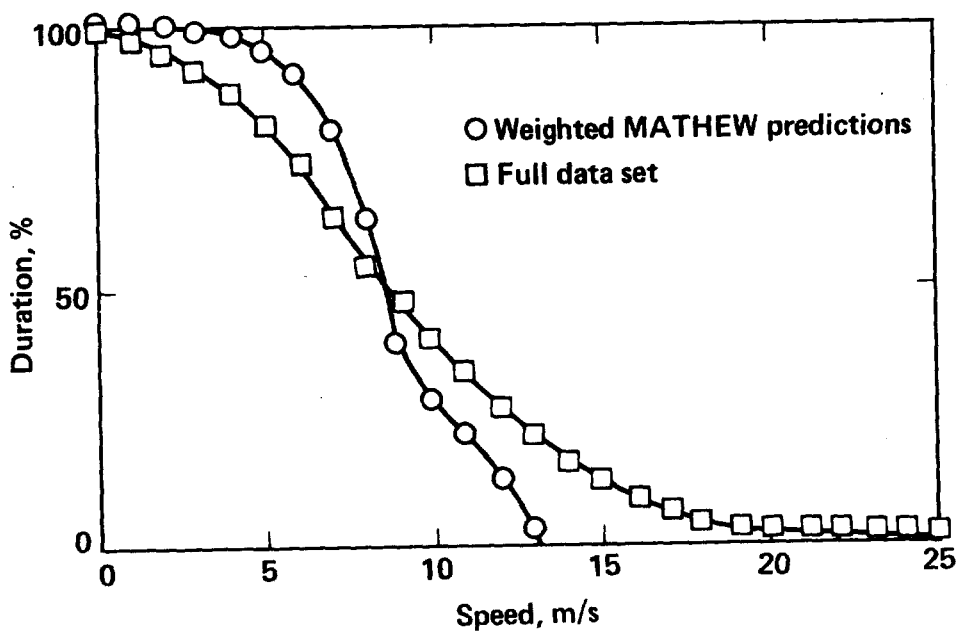

FIG. 32. Wind-speed duration curve from MATHEW/PCA predictions for the Tantalus Tower site, properly located in the terrain (circles), and the duration curve from the full data set (squares).

THE SECOND YEAR'S DATA

The data for August 1977 - July 1978 were analyzed in the same way as those for the period August 1976 - July 1977. PCA first identified the day of each month, and its frequency of occurrence, that best characterized the wind fields for the month. The wind data for each typical day were then input to MATHEW to compute the winds over the entire island. Given the MATHEW computed winds and the frequency of occurrence of each typical day, we calculated annual average wind power for the region at 50 m and determined wind-speed duration curves at the verification sites.

Results from the the first year's data study established that two observations per day were sufficient for meaningful statistics. Therefore, we used only the 2 a.m. and p.m. observations from each typical day as input to MATHEW. With time, fewer stations were providing data to the data base, necessitating some changes in the list of input and verification sites. Of the verification sites used in the first year's work, Kahaku Hill, Honolulu airport, Tantalus Tower, and Kaena Point (30 ft) were retained. The Comsat site was added to this number.

We will begin with a brief discussion of the regional assessment in terms of wind-power contours. Then we will go on to predictions at the verification sites in the form of wind-speed duration curves. In both cases, we will have an opportunity to identify and discuss problems that can affect the validity of results obtained through this kind of analysis.

REGIONAL WIND-ENERGY POTENTIAL

We used the computed winds from the 24 MATHEW runs and the frequency-of-occurrence table from PCA to calculate the annual mean cube wind speed over Oahu at 50 m above terrain. Figure 33 shows the contours, at 50 m, of annual average wind power for August 1977 - July 1978 obtained from these mean cube speeds. The picture is much like that for the first year (Fig. 22), with enhancement along ridge lines and around exposed points of the island. Overall, the strength of the field is slightly less than it was the first year. This is indicated by breaks in the 200-W/m^2 contours along the eastern and western ridges. The 400-W/m^2 contour on the southeast portion of the eastern ridge also lacks the continuity of that calculated for the first year. As we noted in the first year's analysis, the spread of the 200-W/m^2 contours out to the boundaries is a nonphysical artifact of the initial data extrapolation to these areas.

The problem of finding suitabile of data-input sites can be illustrated with the second year's data. Earlier, we showed that realistic wind-field predictions could not be made at Koko Head because the MATHEW averaged topography reduced this site to sea level. For the same reason, Koko Head data were not used as input for the second year's MATHEW runs. Figure 34 shows the effect of trying to use Koko Head for MATHEW input. Except for a broad area of very high values near Koko Head, the contours look much the same as those in Fig. 33. The problem is that MATHEW saw these topographically enhanced winds, observed some 200 m above the ocean, as sea-level measurements. Because this was the only data in the southeast

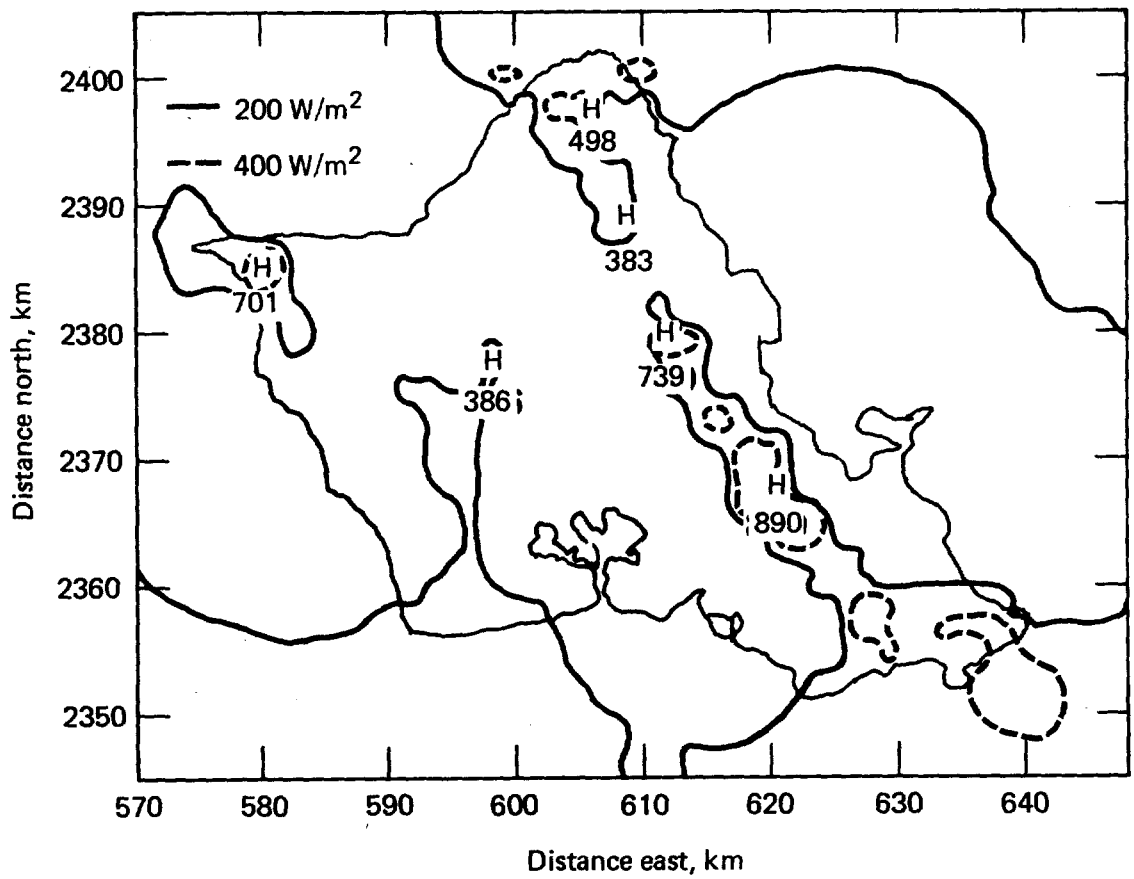

FIG. 33. Predicted annual average wind power at 50 m above terrain for Oahu, Hawaii, for August 1977 - July 1978 based on MATHEW/PCA calculations. Contours are at 200 and 400 W/m^2.

corner of the island, the initial interpolated fields for MATHEW are badly distorted in this area. In fact, the strong power gradients seen in Fig. 34 to the west and north of Koko Head occur where the next nearest sites — Pearl Harbor to the west and Kaneohe MCAS to the north — begin to dominate in the interpolation. On the basis this result, we can state, as a general rule, that a site not resolved in the model topography will not be suitable for wind-field prediction or as a data-input site.

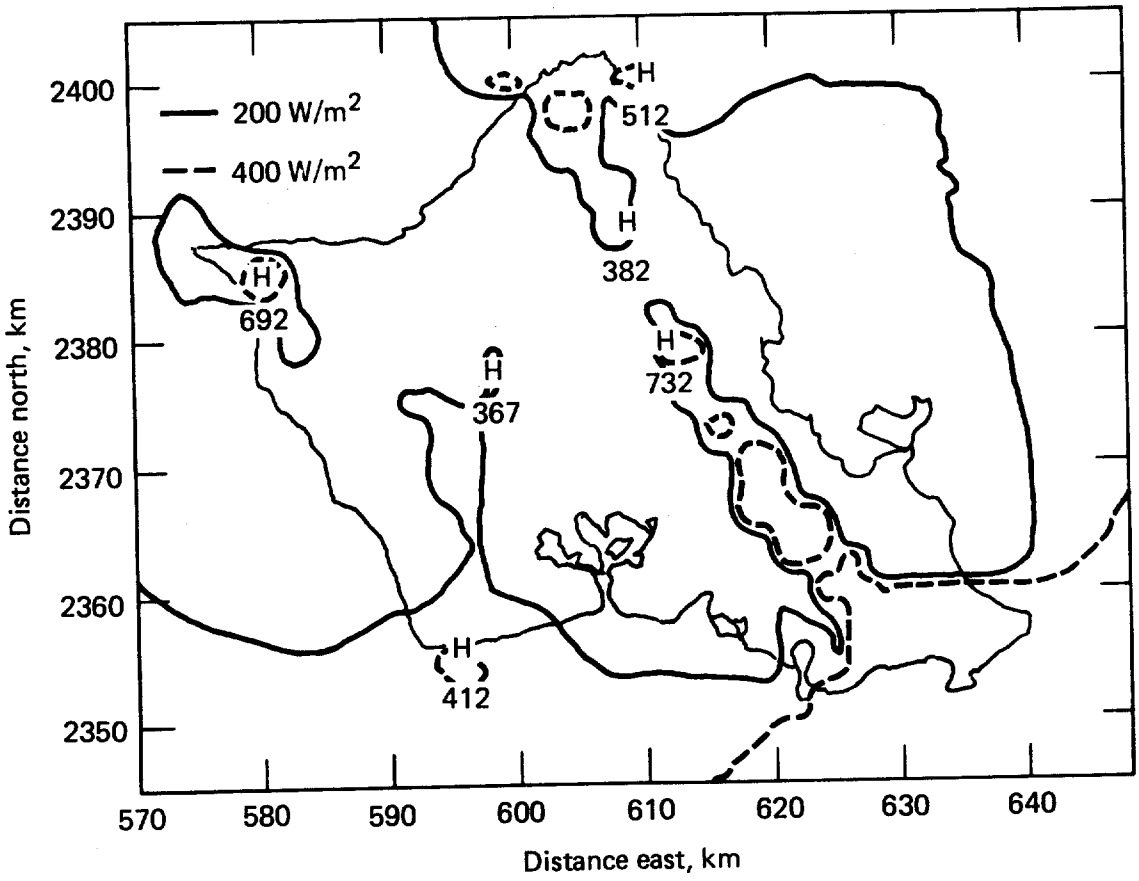

FIG. 34. MATHEW/PCA-predicted annual average wind power at 50 m for Oahu, Hawaii, for August 1977 - July 1978, when data from Koko Head are included. Contours are at 200 and 400 W/m^2.

SITE STATISTICS

Wind-speed duration curves for August 1977 - July 1978 were generated for the five verification sites, using sums of the MATHEW/PCA-predicted winds at these sites weighted by the PCA-determined frequencies of occurrence. Figures 35-39 show these duration curves. In each figure the duration curve, computed using the observed winds at the site, has been included for comparison. Figure 40 shows the MATHEW/PCA-predicted annual mean wind speeds versus those computed from the full August 1977 - July 1978 data set.

From Figs. 35 and 40, we see that the shape of the duration curve for Honolulu airport is fairly well reproduced, while the annual mean wind speed predicted is within 10% of that observed. One would expect a good duration-curve fit here because of the proximity of Honalulu airport to Pearl Harbor, the nearest data input site. A monthly comparison of the wind-speed duration curves for the two locations (Shinn et al) shows a great deal of similarity. The wind-speed duration curve for Tantalus Tower (Fig. 36) shows a steeper drop off than is observed in the data from this site. The failure to produce the long tail of the curve here also occurred in the first year's analysis (Fig. 32). Although it is most evident at the Tantalus site, the phenomenon is present everywhere because we have selected the most-dominant wind field as MATHEW input, thus excluding low-probability extremes of the winds. Predicted annual mean wind speed at Tantalus was about 20% low. Figure 37 shows the duration curve at Kaena Point (30 ft). The corresponding mean wind speed is about 13% greater than that observed; the duration curve fit is not as good as that obtained for the first year (Fig. 14b). We feel, however, that Fig. 14b represents an exceptional result and that Fig. 37 is more representative of the performance of our methodology.

Predictions at the two remaining verification sites, Kakuku Hill and Comsat, were not as good as those for the other three sites. At Kahuku Hill (Fig. 38), we see rather poor agreement between the predicted and observed wind-speed duration curves, although the predicted annual mean wind speed is within 10% of that observed. At Comsat (Fig. 39), the situation is still worse; the predicted and observed duration curves at this site are not even qualitatively alike. Further, predicted annual mean wind speed is a factor of two too high.

In our judgement, there are several reasons for these anomalous effects: In regard to Comsat (Fig. 39), this site lies west-southwest of the region of major terrain enhancement of the wind. The extrapolation of Opana wind (Fig. 41), to Comsat for model input fictitiously attaches a higher wind speed to Comsat than actually existed. In regard to the differences between Opana (Fig. 41), and Kahuku Hill (Fig. 38), we believe that terrain shape factors, unresolved by the model, account for the lack of agreement between velocity duration curves.

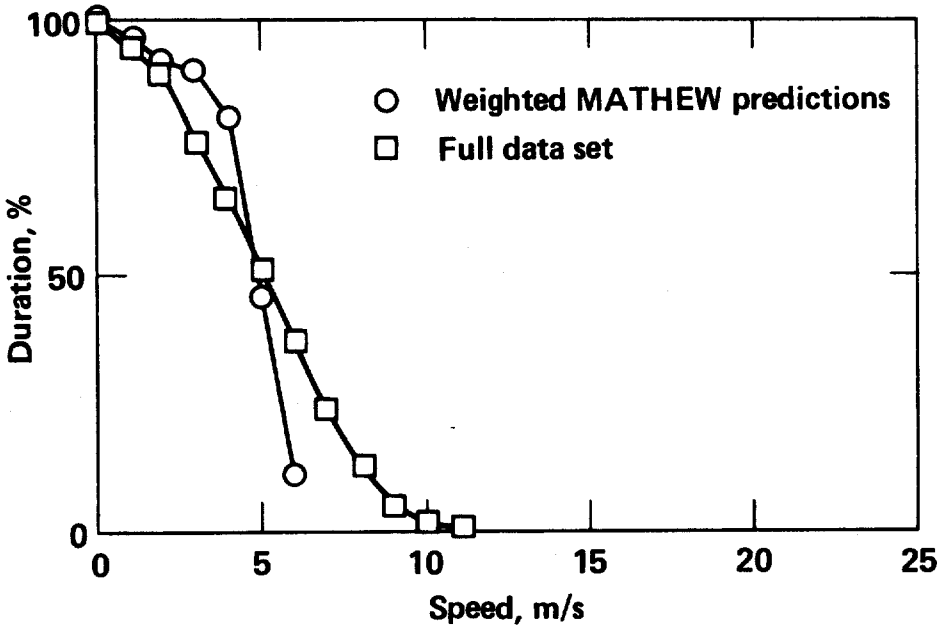

FIG. 35. Wind-speed duration curves at Honolulu Airport for August 1977 - July 1978 from weighted MATHEW/PCA predictions and the full data set.

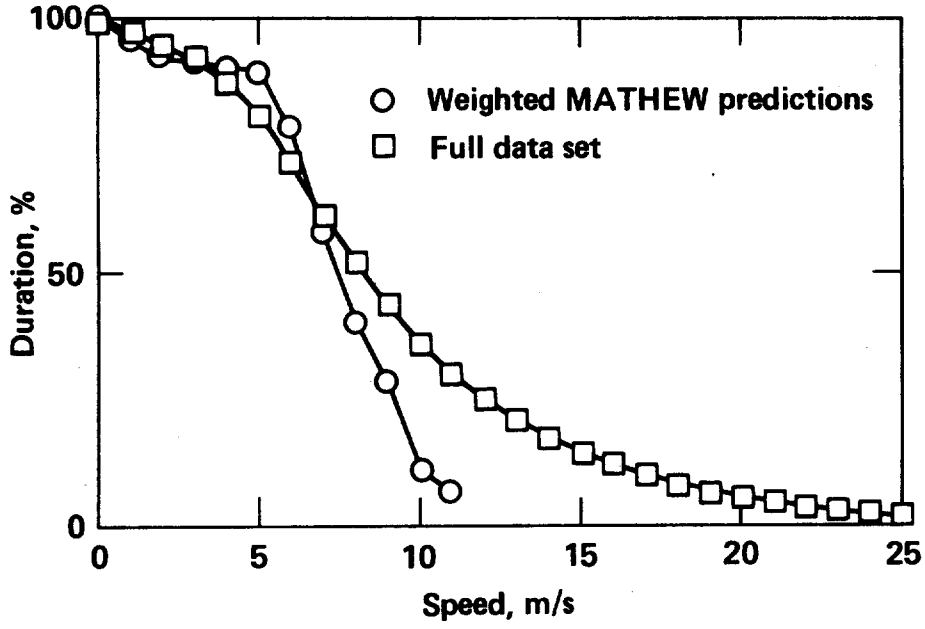

FIG. 36. Wind-speed duration curves at Tantalus Tower for August 1977 - July 1978 from weighted MATHEW/PCA predictions and from the full data set.

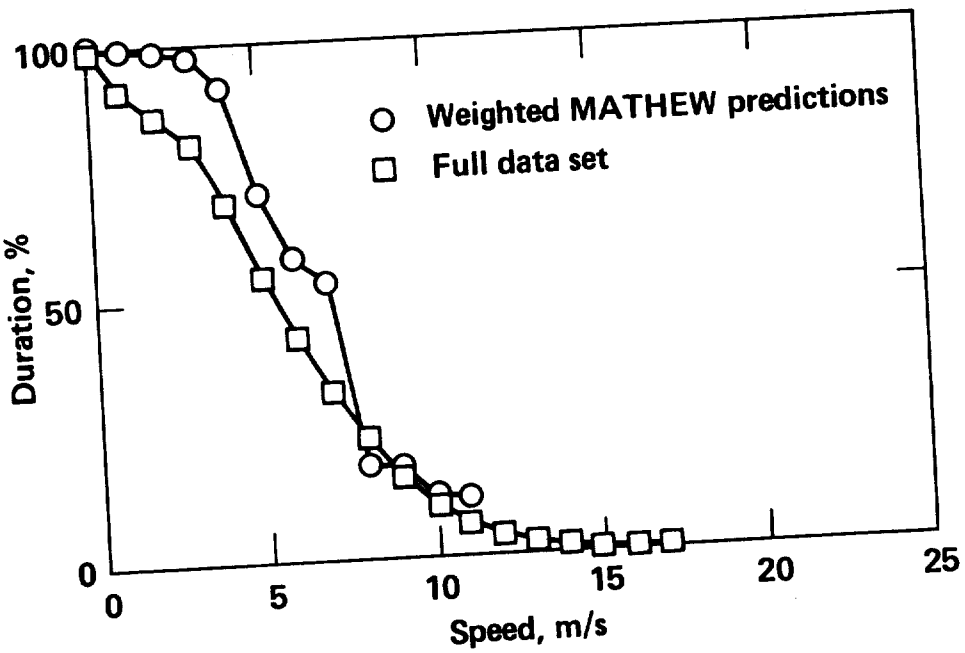

FIG. 37. Wind-speed duration curves at Kaena Point for August 1977 - July 1978 from weighted MATHEW/PCA predictions and from the full data set.

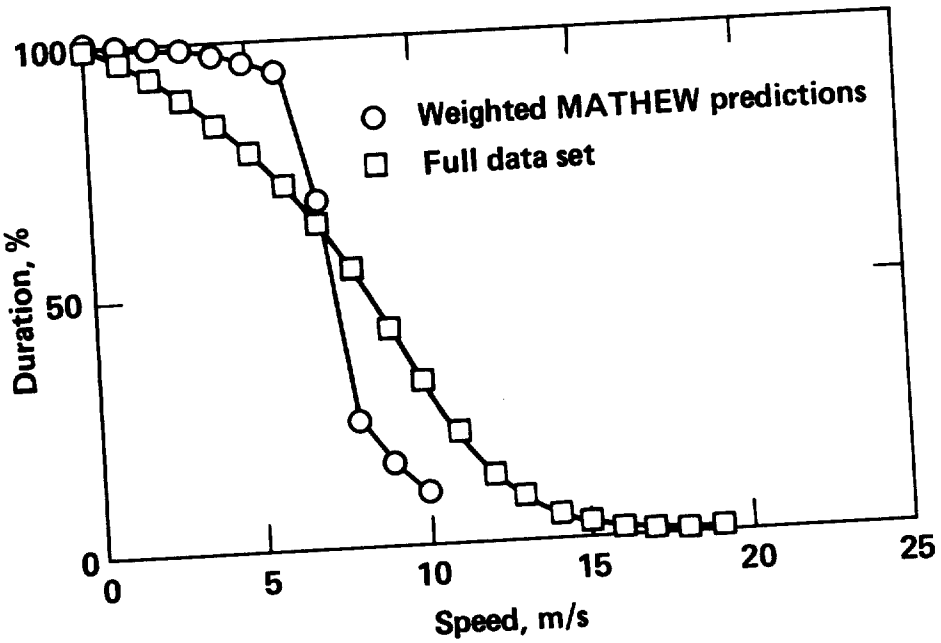

FIG. 38. Wind speed duration curves at Kahuku Hill for August 1977 - July 1978 from weighted MATHEW/PCA predictions and from the full data set.

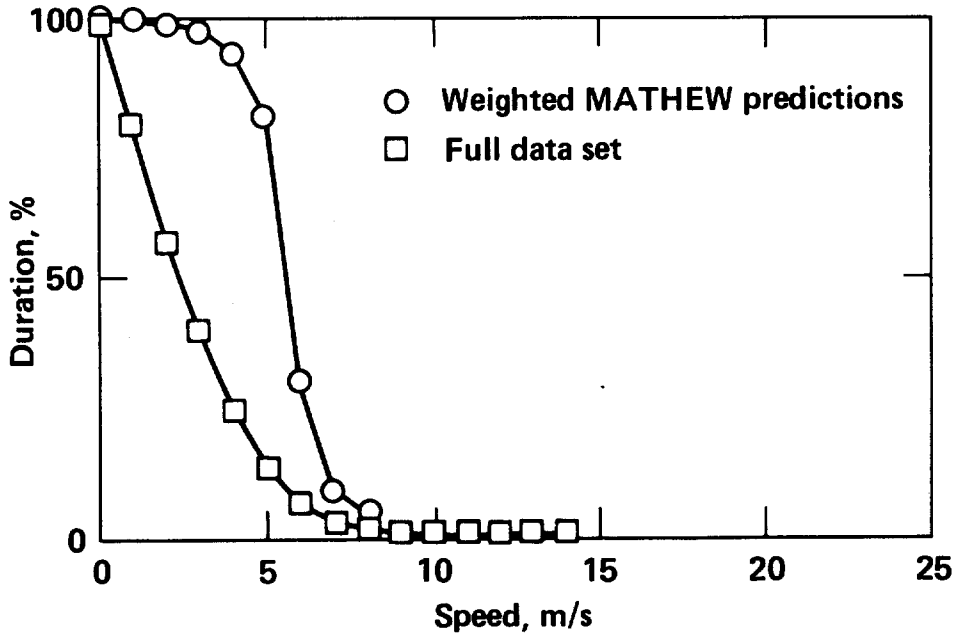

FIG. 39. Wind-speed duration curves at Comsat for August 1977 - July 1978 from weighted MATHEW/PCA predictions and from the full data set.

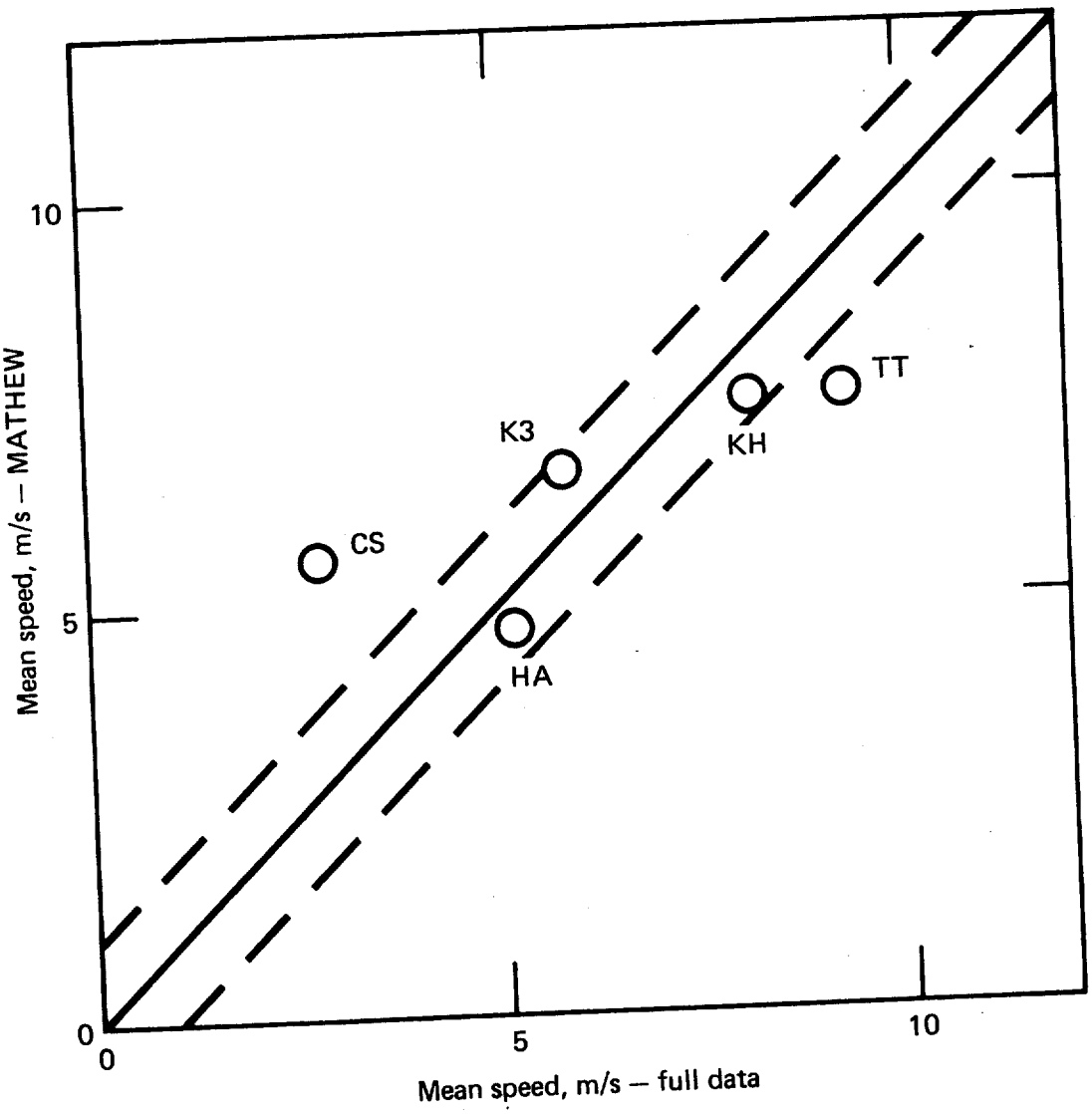

FIG. 40. Annual mean wind speed based on MATHEW/PCA predictions for August 1977 - July 1978 versus that obtained from the full data set. The dashed lines define ± 1-m/s bounds.

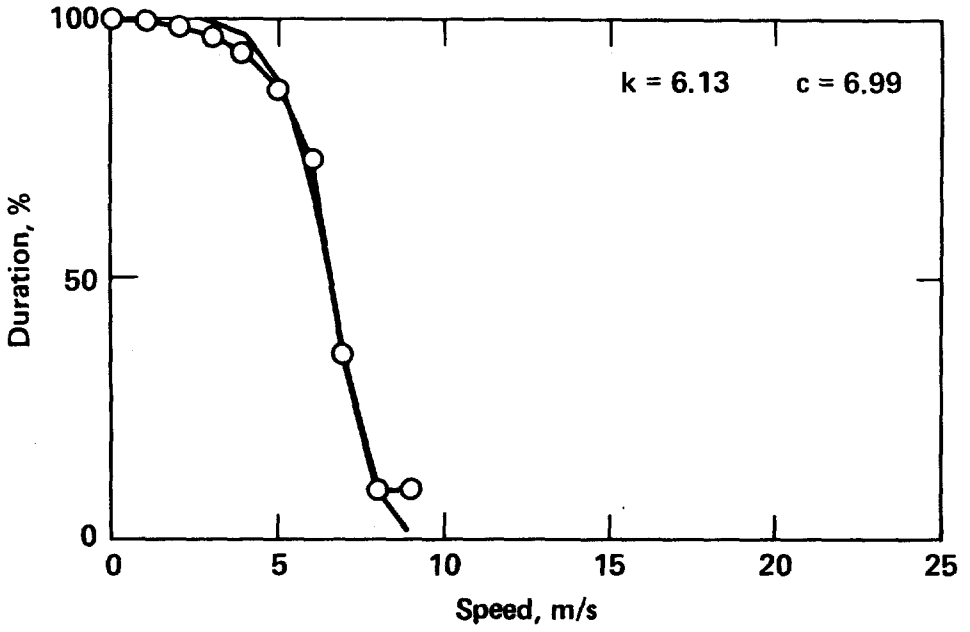

FIG. 41. Wind-speed duration curve at the Kahuku Opana, using all observations at this site for the period August 1977 - July 1978.

From this second-year analysis we may conclude that the methodology has again been able to reproduce both regional and local wind characteristics. However, we must add the strong caveat that any results from this type of analysis will only be as good as our selection of sites for data input and wind-field prediction. Specifically, care must be exercised in the following areas:

- A site for data-input or wind-field prediction must be resolved in the MATHEW-averaged topography. An unresolved, elevated data site will give an initial interpolated field that is too high and that MATHEW will adjust to give erroneously high predictions. At an unresolved prediction site, appropriate terrain enhancement will not be computed and erroneously low wind speeds may be expected.

- Erroneous wind characteristics will be predicted at any site whose initial interpolated winds are dominated by input from a site in radically different terrain.

- A prediction site must be at a point within the MATHEW-averaged topography that is equivalent to its location within the real topography. That is, care must be taken that the topography around the site is not changed through an artifact of the manner in which the MATHEW lower boundary is defined.

MODIFIED MATHEW AND ITS IMPACT ON WIND-ENERGY ASSESSMENTS

In this study, MATHEW was able to simulate such phenomena as deflection of flow around the island, channeling of flow, and wind intensification over the ridges. However, we have recently recognized deficiencies and inconsistencies in the solution methodology of MATHEW. Because of this, we have developed a new version of this code; for convenience, these models will be referred to as old and new MATHEW. Certain attributes of the new MATHEW suggest that its application in future wind power assessments may lead to more accurate results than those previously attainable. Additions and improvements of interest include the following:

1. The new MATHEW has the potential for providing more realistic wind-speed values at noninstrumented positions over the island.

The old MATHEW exhibits a spurious characteristic under low-wind-speed situations, wherein a counter flow (i.e., a flow opposite to the prevailing wind direction) develops along the surface boundary nodes during the adjustment process. Winds important in site selection are generally contained in the layer delineated by these nodes and by the row of nodes immediately above the surface. To estimate winds at points within this layer, we first fit an exponential curve (representing the power-law variation of wind speed in the vertical) to point velocities at the top and base of boundary elements and then extract speeds at specified heights. Obviously, these speeds will tend to be too low when the upper and lower reference velocities are opposite each other. Although testing is still underway, the staggered-grid approach in the new MATHEW (a fundamental difference between the models) appears to eliminate the problem of reverse flow. In this approach, velocities are defined on zone faces, rather than at grid points.

2. Experiments suggest that the new MATHEW produces a more "stable" near-surface solution.

Wind-speed (and direction) values were found to be highly variable and excessively dependent on the relative horizontal position from which they were taken on the boundary cell surface in the old MATHEW, which is a further manifestation of the counterflow problem. In contrast, the new MATHEW is less susceptible to these vagaries; this is again attributable to the staggered-grid formulation.

3. The amount of flow around, as opposed to over, an obstacle can be controlled with a higher degree of confidence.

A highly stable atmosphere inhibits vertical motion. For Oahu, flow tends to be forced around, rather than over, the island's ridges in this situation. From experience gained by modeling various flow regimes, we are able, with Gauss precision moduli, to simulate the phenomenological effect of increasing atmospheric stability on the flow patterns produced by the models. These weights define the allowable horizontal to vertical adjustments on the wind velocities during the mass-consistent calculation. While the old MATHEW has a very narrow range of

response to these parameters, the new MATHEW has a greatly expanded range. The enhanced sensitivity permits us to control and predict the characteristics of the final flow field with a higher degree of certainty.

4. The new MATHEW gives us the option of imposing an impenetrable surface at the top of the grid, wherein we can investigate the effects of an intense, elevated temperature inversion on atmospheric flow.

Northeasterly tradewinds, which persist over the Hawaiian islands 70% of the year, have an associated inversion about 2 km above sea level. Although the intensity of this subsidence inversion varies, it generally forms an effective upper lid, creating a venturi effect in which flow is accelerated over the ridges. A rigid lid in the model mimics an inversion by constraining the winds to be horizontal at grid top. As expected, from consideration of mass-balanced flow, wind velocities near the ridges tend to have magnitudes larger than those without a fixed top and generally agree more favorably with observations.

CONCLUSIONS

This report summarizes the logic steps in the LLL site-screening methodology for wind energy, describes the major elements of PCA regional wind analysis and the diagnostic flow model MATHEW, and illustrates their use within the methodology. The two-year Oahu data base has proved ample for validating the methodology. The success of the methodology is clearly indicated in the results, wherein the mean annual wind speed for independent sites was well predicted by the methodology. It is our conclusion that the site-screening methodology is promising enough to contribute to future regional wind assessments for the DOE.

Further, the site-screening methodology can easily incorporate modeling improvements that will be emerging from the numerical fluid-mechanics community. We have included a discussion of the new MATHEW model and some recently discovered attributes indicated in exploratory, but limited, calculations on the Oahu data base.

The site-screening methodology reported herein is ready for application to other regions rich in wind energy that are awaiting more refined assessment before they can be developed.

ACKNOWLEDGEMENTS

Many people have helped develop and implement the methods discussed in this report. The authors wish to thank M. C. MacCracken and M. H. Dickerson for their guidance in performing the work and preparing the report, T. J. Sullivan, who helped prepare the data for the preliminary assessment, and D. J. Rodriguez, who provided the discussion on the new MATHEW and its attributes emerging from early exploratory calculations on the Oahu data site.

The project could not have begun without data for analysis and verification. Much of the preliminary work on assembling the data base was done by R. L. Zalkan (USN); J. H. Shinn took over these responsibilities in 1976. W. M. Porch helped set up the LLL instrumented sites in the summer of 1976. We owe a particular debt of gratitude to the organizations that provided data. They include the University of Hawaii, the U. S. Navy, Air Force, and Marine Corps and the Comsat Corporation, Honolulu airport, and Pearl Harbor Fleet Weather Central.

D. M. Hardy directed this program from its inception until the fall of 1977. C. A. Sherman directed the program from 1977 until her death on May 16, 1979.

Finally, the authors wish to express their appreciation to DOE technical managers, Lou Divone, and to Carl Aspilden and George Tennyson for their patience during June - December 1979. It was during this period that we attempted to document for our late associate, Christine Sherman, the site-screening methodology for wind energy that was nearing completion at the time of her death. It is our intent that the documentation herein contained suitably reflects the excellence of her contribution to wind energy.

JACjs/1030z/134

U. S. Government Printing Office: 1980/12–789-002/5524

REFERENCES

Essenwanger, O. M., Applied Statistics in Atmospheric Science, Frequencies and Curve Fitting (Amsterdam, Elsevier Scientific Publishing Company) 412 p., Part A (1976).

Hardy, D. M., Empirical Eigenvector Analysis of Vector Observations, Geophys. Res. Let., 4, 319 (1977).

Hardy, D. M. and J. J. Walton, Principal Components Analysis of Vector Wind Measurements, J. Appl. Meteor., 8 1153 (1978).

Justus, C. G., W. R. Hargraves, and Amir Mikhail, Reference Wind Speed and Height Profiles for Wind Turbine Design and Technology, George Institute of Technology report ORO/5108-76/4 (1976).

Justus, C. G., W. R. Hargraves and Ali Yalcin, Nationwide Assessment of Potential Output from Wind-Powered Generators, J. Appl. Meteor. 15 (7), pp. 673-678 (1976).

Knox, J. B., The Wind Resource and Siting Requirements, Solar Energy Technology Handbook, W. Dickinson and P. Cheremisinoff, Eds. published by Marcel Dekker, Incorporated, Part 5, Chapt. 1 (1980).

Knox, J. B., D. M. Hardy, C. A. Sherman, and T. J. Sullivan, Status Report: Lawrence Livermore Laboratory Wind Energy Studies, Lawrence Livermore Laboratory, Livermore, California, UCID-17157, (1976).

Sasaki, Y., An Objective Analysis based on the Variational Method, J. Met. Soc. Jap. 36, 77 (1958).

Some Basic Formalisms in Numerical Variational Analysis, Mon. Wea. Rev. 98, 875 (1970).

Numerical Variational Analysis Formulated Under the Constraints Determined by Longwave Equations and Low-Pass Filter, Mon. Wea. Rev. 98, 884 (1970).

Sherman, C. A., A Mass-Consistent Model for Wind Fields Over Complex Terrain, J. Appl. Meteor. 17, 312 (1978).

Shinn, J. H., C. A. Sherman, J. J. Walton, K. L. Hill, B. R. Clegg, and D. Whisler, Oahu Surface Wind Network Summary of Data, August 1976 through July 1979, Lawrence Livermore Laboratory, Livermore, California, UCID-18232 (1979).

Walton, J. J. and D. M. Hardy, Principal Components Analysis and its Application to Wind Field Pattern Recognition, U.S. Department of Energy, Lawrence Livermore Laboratory, Livermore, California, UCRL-52488, (1978).

Walton, J. J. and C. A. Sherman, Objective Wind Field Pattern Characterization, in Proc. Intern. Tech. Mtg. Air Poll. Modeling Appli., 9th, Toronto, Canada, 1978 UCRL-80901, (1978).